Effect on Pavement Wear of an Increase in Mass Limits for Heavy Vehicles – Stage 2

Transfund New Zealand Research Report No. 231

Effect on Pavement Wear of an Increase in Mass Limits for Heavy Vehicles – Stage 2

J. de Pont, TERNZ Ltd
B. Steven, University of Canterbury
D. Alabaster & A. Fussell, Transit New Zealand

Transfund New Zealand Research Report No. 231

ISBN 0-478-25090-8
ISSN 1174-0574

PO Box 2331, Lambton Quay, Wellington, New Zealand
Telephone 64-4-473 0220; Facsimile 64-4-499 0733

de Pont, J.,[1] Steven, B.,[2] Alabaster, D.,[3] Fussell, A.[3] 2003. Effect on pavement wear of an increase in mass limits for heavy vehicles – Stage 2. *Transfund New Zealand Research Report No. 231.* 49pp.

[1] TERNZ, PO Box 97846, South Auckland Mail Centre, Auckland
[2] University of Canterbury, Private Bag 4800, Christchurch
[3] Transit New Zealand, PO Box 1479, Christchurch

Keywords: accelerated pavement testing, CAPTIF, loading, New Zealand, pavement, pavement loading, pavement performance, road, surface deformation, surface texture, thin-surfaced pavement, texture, traffic, vehicles

An Important Note for the Reader

The research detailed in this report was commissioned by Transfund New Zealand. Transfund New Zealand is a Crown entity established under the Transit New Zealand Act 1989. Its principal objective is to allocate resources to achieve a safe and efficient roading system. Each year, Transfund New Zealand invests a portion of its funds on research that contributes to this objective.

While this report is believed to be correct at the time of its preparation, Transfund New Zealand, and its employees and agents involved in its preparation and publication, cannot accept any liability for its contents or for any consequences arising from its use. People using the contents of the document, whether directly or indirectly, should apply, and rely on, their own skill and judgement. They should rely on its contents in isolation from other sources of advice and information. If necessary, they should seek appropriate legal or other expert advice in relation to their own circumstances, and to the use of this report.

The material contained in this report is the output of research and should not be construed in any way as policy adopted by Transfund New Zealand but may form the basis of future policy.

Contents

Executive Summary

Introduction

The road transport industry in New Zealand has been lobbying for increases in the allowable mass limits for heavy vehicles on the basis that increases would lead to increased efficiency and benefits to the economy. Some of the proposals for increased mass limits involve increased axle load limits, which would clearly lead to additional pavement wear. Road controlling authorities, while sharing the industry's aims for increased efficiencies in the road transport system, are concerned that any additional pavement wear generated by higher axle loads is paid for, so that the standard of the road network can be maintained.

Under the current road user charges regime the users would be charged for the additional wear on the basis of the fourth power law, which states that the amount of damage caused by the passage of an axle is proportional to the fourth power of its weight. Thus an axle load increase of 10% would lead to an increase in road user charges for that axle of 46%. This fourth power law has its origins in the AASHO road test which was conducted in the United States in the late 1950s using roads and vehicles which bear little resemblance to those in use in New Zealand today.

Pavement Testing

To determine the effects of increases in mass limits on pavement wear, a multi-stage accelerated pavement testing programme was undertaken between 1999 and 2001 at the Canterbury Accelerated Pavement Testing Indoor Facility (CAPTIF). This report documents Stage 2 of the project carried out during 2000/2001, and primarily investigates the effect of increase in mass limits of heavy vehicles on the life of a chipseal surfacing.

Stage 1, undertaken during 1999/2000, investigated the effect of increase in mass limits on pavement life of four pavement sections that differed only by aggregate type. For comparing the effects of an increase in mass limits at CAPTIF, two "vehicles" which are known as SLAVEs (Simulated Loading and Vehicle Emulators) were configured with identical suspensions but with different axle loads. One was loaded to 40 kN to simulate the current 80 kN axle load limit, while the other was loaded to 50 kN to simulate a possible increase to a 100 kN axle load limit. The test was conducted with the two SLAVEs trafficking parallel independent wheel paths so that the relative wear generated by the two could be compared.

Comparisons of the Wear Models

To relate the findings on surface texture wear back to the earlier work in Stage 1 on Vertical Surface Deformation (VSD), some additional analysis and modelling of the VSD changes were undertaken. Thus comparisons between the two forms of wear can be made. The important findings are listed below.

Texture Models

- The measurement of texture depth has a great deal of variability and it needs to be averaged over a large number of readings to get stable results. Thus getting sensible trends in texture depth changes was not possible by comparing the readings at one measurement station at different numbers of load cycles. The averages had to be taken around a complete cycle of the track.

- Two models for texture change (the Patrick and Cenek models) which are used for pavement performance prediction in New Zealand do not account well for the effect of mass. These models, which are essentially identical but formulated differently, can be adjusted to match the measured data well, although using coefficients that differ significantly from those given by either Patrick or Cenek.

- A Compaction-Wear model of the form developed for VSD in Stage 1 of this project can be fitted to the texture change data. But because the rate of change of mean profile depth does not appear to become constant, this form of model does not fit the data as well as the Patrick and Cenek models.

- A modification of the form of model used by two researchers in Australia, Kinder and Lay, to model surface deformations was fitted to the texture data and resulted in a superior fit to that of the Patrick and Cenek models. As the Kinder-Lay model explicitly accounts for the effect of mass with a power law relationship, it is also much more useful for the aims of this study. The best-fit exponent of the power law for the effect of mass was 1.69.

VSD Models

- The Kinder-Lay form of model was then fitted to the VSD data which had previously been analysed in the Stage 1 report. Fitting models to each of the four pavement segments independently generated good fits, although the fit was not as good as the original Stage 1 Compaction-Wear models. However, the model coefficients for the different segments differed radically from each other even though the pavements were actually quite similar. This severely limits the potential usefulness of these models as a predictive tool because the coefficients cannot easily be determined in advance.

- A single Kinder-Lay model was then fitted to the data for all four segments. This is a much more usable model but did not fit the measured data well for all four pavement segments.

- The Compaction-Wear model developed in Stage 1 had only been fitted to the four segments independently. In Stage 2 a single Compaction-Wear model was fitted to all four pavement segments simultaneously. Although not perfect, this gave a better fit than the Kinder-Lay form of model. The embedded power law term for the effect of mass in this model had an exponent of 1.8.

- The Compaction-Wear model does not account for the load cycles needed to achieve the compaction and thus does not match the initial load cycles well. A blending function with a clear physical interpretation was developed to model this compaction phase and it worked very well.

General Form of Models

- As found in Stage 1, the Compaction-Wear model implies that an increase in mass will result in both additional compaction and additional wear with the effect that an apparent rapid degradation will occur in the condition of the network. Some experimental support for this hypothesis was shown in the measurements undertaken on the pavement in this Stage 2 of the study.

  The modified Kinder-Lay model used to predict the texture changes does not include an effect similar to this compaction. This does not mean it will not occur but the model cannot predict it, and no experiments have been done that specifically test this hypothesis.

- For both compaction and wear, the power law for the effect of mass has an exponent of just less than 2.

The results should only be interpolated, and should not be extrapolated, outside the range of axle loads that were tested. That is, a power 2 relationship between the 8.2 tonne and 10 tonne axles may not mean that a power 2 relationship can be applied for comparing 6 tonne and 8.2 tonne axles).

Further Investigations

From these findings, some questions for further investigations arise.

- Further experimental validation of the Compaction-Wear model is required. Ideally a pavement at CAPTIF should be loaded at a lower load level until the linear rate of VSD progression is achieved. The load should then be increased and testing continued until the rate of change of VSD stabilises again. This load increase could then be repeated. If the Compaction-Wear model is valid, each load increase should result in additional compaction and an increased wear rate.

- The surface texture should also be tested in a similar manner to VSD, and the modified Kinder-Lay model for texture should be validated. If the texture change is a two-stage process like the Compaction-Wear model for VSD, this test will show it.

- Both models have a constant coefficient, K, which depends on the pavement properties. Further work is required to develop methods for predicting the K values from the pavement material properties.

Applying Pavement Wear Models

Although the Compaction-Wear model may not appear to be substantially different from the power law model currently used, it has major implications if applied to a user-pays regime of road funding.

With the Compaction-Wear model a significant part of the total VSD comes from the compaction component, which depends on the axle loads but not significantly on the number of load cycles applied.

The compaction component occurs immediately post-construction and therefore the total annual sum collected for compaction should reflect the total compaction that will occur with pavements constructed in that year.

The wear component is based on the number of load cycles and hence could be collected as road user charges.

Both these components are related to approximately the second power of load rather than the fourth power, which means that the relative damage caused by larger trucks with high axle loads would be less than those currently assumed. In the longer term, we would be likely to see a change in the mix of vehicle configurations in the heavy vehicle fleet.

Because this would have a major impact on the road transport industry it is important to ensure that the Compaction-Wear model is suitably validated.

Abstract

To improve the efficiency of the road transport industry in New Zealand, a range of mass limit increases for heavy vehicles has been proposed. Some of the options for mass increases include increasing the axle load limit, which would inevitably lead to increased road wear. As New Zealand has a mass-distance road user charging regime where the users pay for the road wear they generate, this increased wear is in itself not a problem provided that the charges accurately reflect the wear. At present, road user charges are based on the fourth power law, which was developed from the AASHO road test carried out in the United States in the 1950s. The pavements and vehicles used for that test differ considerably from those in use in New Zealand today.

To determine the effects of increases in mass limits on pavement wear, a multi-stage accelerated pavement testing programme was undertaken at the Canterbury Accelerated Pavement Testing Indoor Facility (CAPTIF) between 1999 and 2001. Stage 1 investigated the effect of increase in mass limits on pavement life on four sections that differed only by aggregate type. This report documents Stage 2 of the project and investigates the effect of increase in mass limits on the life of a chipseal surfacing. For comparing the effects of an increase in mass limits, the axle load on one wheel path was 80 kN, while the load on the other was increased to 100 kN.

1. Introduction

1.1 Background

The road transport freight industry understandably wishes to increase its efficiency. One of the ways to do this is to increase the allowable mass limits for heavy vehicles. This in turn can result in economic benefits to the whole country provided that the impact of the changes in mass limits are accurately known and considered in assigning the new limits and in determining appropriate road user charges. One of the impacts concerning road-controlling authorities is the effect of increasing mass limits of heavy vehicles on the life of their pavements, or how much more pavement rehabilitation and maintenance will be required.

In response to the industry's requests for larger and heavier vehicles, Transit New Zealand has recently undertaken a study to assess the economic and safety impacts of increasing mass limits. This study investigated two scenarios:

- Scenario A, where heavier vehicles subject to the same dimensional limits that are currently in place would be permitted to operate across the entire network, and
- Scenario B, where longer and heavier vehicles would be permitted to operate only on a selected set of key routes.

Within these two scenarios, several axle mass limit options as shown in Table 1.1 were considered.

Table 1.1 Axle mass limit options in Transit New Zealand Heavy Vehicle Limits project.

Option	Allowable weights (tonnes)			
	steer axle	single axle	tandem axle	triaxle
Present	6.0	8.2	15	18
1	6.0	8.2	15	19
2	6.0	8.2	15	20
3	6.0	8.8	16	20

Transit New Zealand's evaluation of these proposed changes in mass limits included research into the safety, geometric, and economic impacts on pavements and bridges. In determining the pavement wear impact of these mass limits changes, existing theories for the relationship between vehicle loads and pavement wear were applied. The most widely used existing theory for determining the effect of mass limit increases on pavement life is the fourth power law. This is used to determine the pavement loading as a number of Equivalent Standard Axles (ESAs). The formula for converting an actual axle load to ESA is:

$$\text{ESA} = \left[\frac{\text{Actual axle load}}{\text{Reference axle load}} \right]^4$$

This fourth power relationship between axle loads and pavement life has never been validated for New Zealand's thin-surfaced unbound granular pavements. It had its origins in the AASHO[1] road test which was conducted in the United States in the late 1950s. It was carried out on roads and vehicles which bear little relationship to those in use in New Zealand today.

Since then, power values between 1 and 8 have been suggested by different researchers throughout the world for different pavement structures and failure mechanisms (Cebon 1999, Kinder & Lay 1988, Pidwerbesky 1996). Even the AUSTROADS Pavement Design Guide, which is the basis of New Zealand design practice, uses a power of 4 for unbound basecourse performance and a power of 7.14 for subgrade performance.

The use of a fourth power relationship predicts that the 7.3% increase in allowable loading for a single axle as per option 3 (Table 1.1) will result in a 33% increase in pavement wear. Should this increase in pavement wear occur, a road controlling authority can expect a 33% increase in the length of pavement rehabilitation required per year to maintain the road network to the same standard. The actual situation is not as extreme as this because, in the first place, not all vehicles will change to the higher limits, and second, the higher axle load limits will result in higher payloads and consequently fewer trips for the same freight volume. Nevertheless, a change to option 3 (Table 1.1) will represent a significant increase in annual expenditure on roads for a road controlling authority and requires budgeting for. The uncertainty in the validity of the fourth power rule poses difficulties when requesting increases in funding for the next financial year. Justifying an increase in the road user charges based on a fourth power rule that has not been validated in New Zealand is expected to be increasingly difficult, particularly as research results from accelerated pavement tests are suggesting different relationships.

The study reported here is Stage 2 of a multi-stage accelerated pavement testing programme that is investigating, using pavement testing on typical New Zealand pavement designs, the relative effect on chipseal surface life in terms of mean texture depth of an increase in axle load from 8.2 tonnes to 10 tonnes. The effect of pavement life in terms of vertical surface deformation (VSD) for the same increase in axle load was completed as part of Stage 1. The results of Stage 1 are reported in de Pont et al. (2001) but are re-visited in this report as similar trends are observed between the effects of pavement and surfacing life. The 10-tonne axle used in this research is somewhat higher than the proposed limit in option 3 (Table 1.1). There are two reasons for using this higher axle load. The first is that, in response to the heavy vehicle limits study, the bus and coach industry has suggested that this level of increase should be considered. The second is that the larger mass difference between the two wheel paths is more likely to ensure that the difference in wear is sufficiently large to be able to draw clear conclusions. By interpolating the results of this research, the effect on pavement life of loading increases should be possible to assess directly (without necessarily using any power law).

[1] AASHO, American Association of State Highway Organisations which, in 1974, became AASHTO, American Association of State Highways & Transportation Organisations.

A key issue for this study is what constitutes pavement wear. The OECD DIVINE project (OECD 1998) differentiates between functional and structural condition for pavements. Functional condition reflects the ability of the pavement to provide service to the road user and covers factors such as roughness, rutting and skid resistance. Structural condition relates to the ability of the pavement to support the loads applied to it and relates to cracking and other forms of distress. In some instances a loss of functional condition may also indicate a loss of structural condition. In New Zealand pavement maintenance and rehabilitation is driven primarily by measures of functional condition and thus, in Stage 1 of this study, the measure of wear considered was the vertical surface deformation while for Stage 2 it was the mean texture depth.

1.2 The Canterbury Accelerated Pavement Testing Indoor Facility (CAPTIF)

The CAPTIF facility is located in Christchurch, New Zealand. It consists of a 58 m-long (on the centreline) circular track contained within a 1.5 m deep x 4 m-wide concrete tank, so that the moisture content of the pavement materials can be controlled and the boundary conditions are known. A centre platform carries the machinery and electronics needed to drive the system. Mounted on this platform is a sliding frame that can move horizontally by one metre. This radial movement enables the wheel paths to be varied laterally and can be used to operate the two "vehicles" in independent wheel paths. An elevation view is shown in Figure 1.1.

At the ends of this frame, two radial arms connect to the Simulated Loading and Vehicle Emulator (SLAVE) units shown in Figure 1.2. These arms are hinged in the vertical plane so that the SLAVEs can be removed from the track during pavement construction, profile measurement, etc., and in the horizontal plane to allow vehicle bounce.

CAPTIF is unique among accelerated pavement test facilities in that it was specifically designed to generate realistic dynamic wheel forces. All other accelerated pavement testing facility designs, that we are aware of, attempt to minimise dynamic loading. The SLAVE units at CAPTIF are designed to have sprung and unsprung mass values of similar magnitude to those on actual vehicles and use, as far as possible, standard heavy vehicle suspension components. The net result of this is that the SLAVEs apply dynamic wheel loads to the test pavement that are similar in character and magnitude to those applied by real vehicles. A summary of the characteristics of the SLAVE units is given in Table 1.2. The configuration of each vehicle, with respect to suspensions, wheel loads, tyre types and tyre numbers, can be identical or different, for simultaneous testing of different load characteristics.

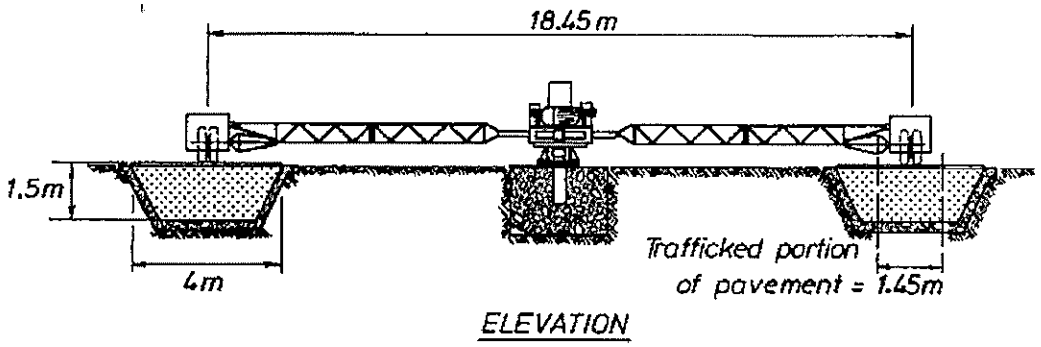

Figure 1.1 Elevation view of CAPTIF.

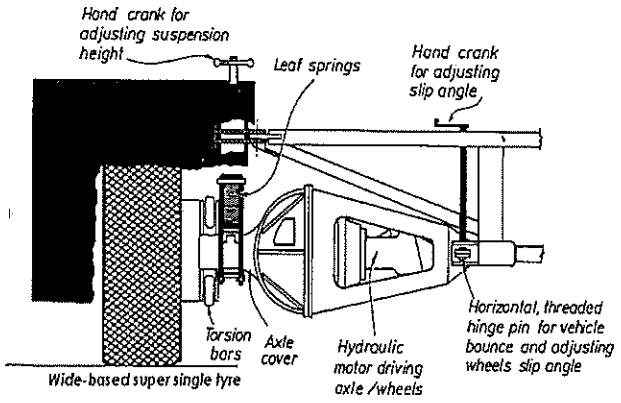

Figure 1.2 The CAPTIF SLAVE unit.

Pavement instrumentation which can be used at CAPTIF includes: Emu coil transducers for measuring vertical, longitudinal and transverse strains in the basecourse and subgrade layers of the pavement; H-bar strain gauges for measuring horizontal strains at the bottom of the asphalt layer; and partial depth gauges for measuring the pavement layer deflections. As well, temperature probes are used to monitor both the pavement and air temperatures. The vehicle instrumentation consists of accelerometers mounted on both the sprung and unsprung masses of each "vehicle" and displacement transducers to measure suspension displacements. As the "vehicle" is a fairly simple quarter vehicle structure, dynamic wheel forces can be calculated by combining the two accelerometer signals weighted by appropriate mass factors.

Other measurement systems used at CAPTIF during testing are: a Falling Weight Deflectometer (FWD); a Loadman Falling Weight Deflectometer; the CAPTIF Deflectometer, which is a modified Benkelman Beam; a transverse profilometer; a DIPStick profiler; a longitudinal laser profilometer; and a stationary laser profilometer. The stationary laser profilometer is used to measure surface texture. For measurement convenience the track is divided into 58 equally spaced stations which are 1 m apart on the centreline wheel path.

A more detailed description of the CAPTIF and its systems is given by Pidwerbesky (1995).

Table 1.2 Characteristics of the SLAVE units.

Test wheels	Dual- or single-tyres; standard or wide-base; bias or radial ply; tube or tubeless; maximum overall tyre diameter of 1.06 m
Mass of each vehicle	21 kN to 60 kN, in 2.75 kN increments
Suspension	Air bag; multi-leaf steel spring; single or double parabolic
Power drive to wheel	Controlled variable hydraulic power to axle; bi-directional
Transverse movement of wheels	1.0 m centre-to-centre; programmable for any distribution of wheel paths
Speed	0-50 km/h, programmable, accurate to 1 km/h
Radius of travel	9.2 m

1.3 The Test Programme

This report follows from the 1999/2000 Stage 1 research reported by de Pont et al. (2001). The pavement constructed in the original 1999/2000 project was utilised for the three tasks of the Stage 2 research carried out in 2000/2001.

Task 1
In the first task of the 2000/2001 research, stresses and strains were measured within the pavement for a range of tyre types, loads and pressures. During this work an additional 19,000 cycles of loading were applied to the original pavement. The work was performed as part of an AUSTROADS research programme and has been reported by Vuong & Sharp (2001). From the load response data, an accelerated pavement test programme was developed for CAPTIF and ALF (Accelerated Loading Facility) for the 2000/2001 year.

Task 2
In the second task of the 2000/2001 research, the mass of the 8.2-tonne vehicle used in the 1999/2000 research was increased to 10 tonnes, and a further 300,000 load cycles were applied. This was undertaken to examine how the rate of rutting on an existing pavement would change with the application of a heavier load. The results of this task were included in de Pont et al. (2001) but are further analysed here.

Task 3
In the third and final task of the 2000/2001 research, which this report is predominantly about, the track was rehabilitated, re-surfaced with a chipseal, and tested using both the 8.2-tonne and 10-tonne simulations. The loads were in separate wheel paths to provide a direct comparison of loss of surface texture.

2. Objectives

The objectives to be achieved by the overall research programme funded by Transfund New Zealand and AUSTROADS are as follows:

1. To determine the relative damaging effect on pavement wear and chipseal life compared to the standard load (8.2-tonne dual-tyred single axle) for increases in vehicle loads and tyre pressures by applying accelerated testing, load response data, existing accelerated pavement test results, and the use of an appropriate pavement model.

2. To determine appropriate road user charges for new heavy vehicle load limits that take into account their effect on both pavement and chipseal life.

3. To provide a methodology and pavement model to predict the potential impact on the road network caused by increases in heavy vehicle load limits.

The five specific objectives to be achieved in the 2000/2001 Stage 2 research are:

1. To measure the pavement response (stresses and strain) for a range of tyre types, loads and pressures.

2. To determine an appropriate pavement model to predict life.

3. To predict pavement life from the pavement response data using an appropriate pavement model.

4. To determine the effect on pavement rutting on an already trafficked pavement when the axle loading is increased from 8.2 tonnes to 10 tonnes.

5. To determine the relative effect on chipseal life between an 8.2-tonne and a 10-tonne dual-tyre single-axle load.

The first three of these objectives were targeted in Task 1 of the 2000/2001 research. The work was funded by AUSTROADS and is described in Vuong & Sharp (2001). The fourth objective was targeted in Task 2 of the 2000/2001 research (and based on the 1999/2000 research reported in de Pont et al. 2001). The fifth objective was met in Task 3 of the test programme, and this report records the results. (Tasks 1, 2 and 3 are described in Section 1.3 of this report.)

3. Method

3.1 Pavement Design

The objective of the original 1999/2000 pavement design was to replicate the relatively low levels of rutting observed in typical New Zealand pavements while maintaining a balance between the life of the heavily loaded (10 tonne) outer wheel path and the lightly loaded (8.2 tonne) inner wheel path.

The decision to use four sections of differing materials was made to accommodate the requirements of another project that also used data from the 1999/2000 test (Arnold et al. 2001). The original experimental design called for only one pavement material. The four pavement sections were not considered separately in the original design as insufficient data was available. Also pavements of the same depth were considered to be preferable, in order to limit the number of variables in the project.

The pavement was designed in an iterative manner using the AUSTROADS Pavement Design Guide (1992). The iterative designs assumed a 700 kPa tyre pressure with a 95.6 mm-tyre radius on the inner wheel path, and a 850 kPa tyre pressure with a 97 mm-tyre radius on the outer wheel path. The basecourse layer was, from previous experience, modelled with a modulus of 400 MPa using AUSTROADS sub-layering and, as convention dictates, the thin asphaltic layer was not considered in the analysis. The subgrade was modelled with a 10^{th} percentile design in-situ CBR[2] of 10, based on test results at the top of the subgrade layer, and used the standard 10 times CBR relationship to obtain the modulus.

The iterative analysis suggested that the inner (8.2 tonne) wheel path would require a basecourse depth of 250 mm to withstand the design 1 000 000 wheel passes, and a depth of 290 mm for the outer wheel path, assuming the AUSTROADS subgrade strain criterion. Using the fourth power law to convert the 10-tonne wheel to an equivalent number of standard axles, rather than modelling directly, suggested that the outer wheel path would need to be 270 mm deep.

The final design using 275 mm basecourse resulted in a pavement that, in the inner wheel path, would theoretically fail at 2 900 000 wheel passes, and at 600 000 wheel passes in the outer wheel path, assuming the AUSTROADS subgrade strain criterion and directly modelling the tyres. Using the fourth power law suggested that the outer wheel path would fail at 1 200 000 wheel passes.

3.2 Chipseal Design

Chipseals are relatively untried at CAPTIF, and the last known trial over ten years ago was believed to have been hand-sprayed. As part of the chipseal surfacing design a meeting was held with the sealing contractor to discuss possible chipseal surfacings to apply in the CAPTIF environment.

[2] CBR – California Bearing Ratio, a test to measure soil strength.

The likely difficulties of the CAPTIF environment were discussed, and included:

- The tight radius creating turning stress on surfacings, and in particular leading to scuffing on the outer tyre track of dual-tyred axles.
- The tight radius presenting difficulties for even application of bitumen and chip.

The benefits of the CAPTIF environment were also discussed, and included:

- The ability to control initial trafficking speed, load and rolling pattern.
- No risk of rain damaging the seal.

The solution was to design a robust seal able to withstand turning stress, and ensuring that the conditioning and loading of the seal is carefully controlled. Bitumen was to be applied with the CAPTIF spray bar, which is designed for applying a constant application rate over the width of the circular track.

The design chosen was:

- Basecourse surface to be lightly prime sealed (approx. 0.2 ℓ/m^2), with a 50/50 blend of 80/100 bitumen and a turpentine cutter.
- After the turpentine evaporated, a Grade 4 seal to be applied using 80/100 bitumen with adhesion agent and no cutters.
- The Grade 4 seal, on completion of the construction rolling, to be conditioned by SLAVE with a single-tyre single-axle minimum loading, and a uniform loading pattern at low speed.
- After the Grade 4 seal, a Grade 3 & 5 two-coat seal to be applied using 80/100 bitumen, with adhesion agent and a minimum of cutters, and conditioned as for the Grade 4 seal.
- Final pavement loading to be with a single-tyre single axle, with wander in the wheel path. The rate of loading to be monitored to ensure that unnecessary damage to the seal did not occur during the early load cycles.

Further discussion with peer reviewer John Patrick of Opus Central Laboratories, Lower Hutt, confirmed that the single-tyre single-axle loading would be appropriate to simulate a dual-tyre single-axle load.

In the event of premature flushing two possible contingencies were discussed. They were water blasting the surface and resealing, or completely removing the seal and sealing from the basecourse again. The water blasting was the preferred plan as it is simpler, quicker and has been demonstrated to work in the field. The seal removal option would require considerably more time. Stripping was not considered likely given the controlled environment.

3.3 Pavement Construction

This section describes the re-surfacing of a pavement previously constructed and trafficked at CAPTIF. The original 1999/2000 pavement construction, which was used for Stage 1, and Stage 2 Tasks 1 and 2 of the project, is described in de Pont et al. (2001), and shown in Figure 3.1.

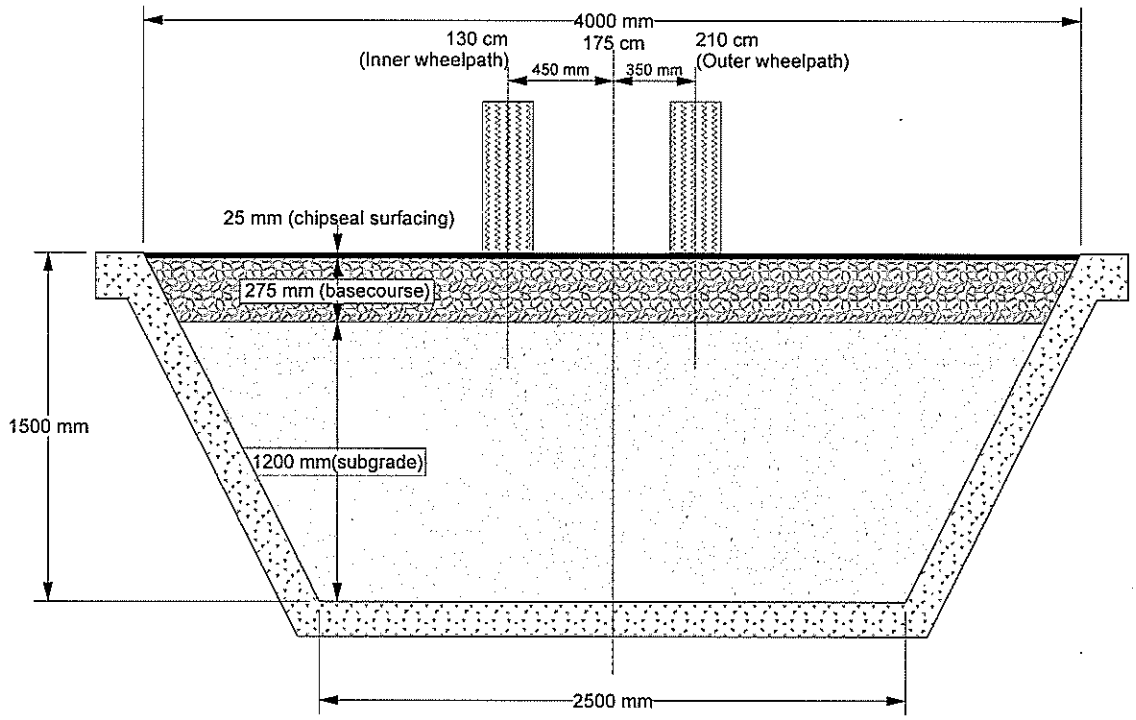

Figure 3.1 CAPTIF pavement cross section and wheel path locations.

3.3.1 Basecourse Construction

The asphalt surfacing of the original pavement was removed and the post-mortem trenches were backfilled and compacted. The basecourse surface was ripped by a backhoe digger to a shallow depth and then topped up with approximately 75 mm of the different parent materials. A tractor with a laser-controlled blade cut the surface back to the target level, and a 3-tonne steel/rubber combo roller was used for compaction. The result was a very accurate surface finish within ±6 mm of design level. The cutting action removed any loose or boney material from the surface, and resulted in very good basecourse density.

The basecourse surface, once dry, was swept by power-broom and primed by hand lance. The basecourse surface texture was measured at the three primary stations in each segment for both inner and outer wheel paths with the Stationary Laser Profilometer. The basecourse surface was also measured for hardness using the "Ball Bearing" surface hardness test.

3.3.2 Chipseal Application

The contractor successfully fabricated the new spray bar to CAPTIF specifications, and calibration was carried out on a simulated test track in the contractor's yard. The binder application at CAPTIF was a success, though the speed required for the sprayer truck was rather high for the confines of the test track. Chip was spread with a standard spreader truck, with the gates on the roller feed adjusted for the radius of the track.

A steel/rubber combo roller pressed the chip in and was generally effective but the surface in Segment C (using Montrose rock for basecourse) failed under rolling. Stationary Laser Profilometer readings on the first coat seal were taken. Basecourses used for Segments A and B were based on AP40 TNZ M/4 aggregate, and for Segment D it was recycled concrete.

The failed Segment C surface was removed and replaced by 25 mm of asphaltic concrete. The second coat of the two-coat seal using Grade 3 chip, followed by more binder and a Grade 5 chip, was applied to all but the asphalt section. The surface was swept and vacuumed by a suction truck.

The final construction of the chipseal surfacing, as listed here, reflects that the seal was applied late in the sealing season:

- Prime Coat 50/50 Bitumen/Turpentine cutback, hand sprayed at approx. 0.3 λ/m^2 to leave approx. 0.15 λ/m^2 residual.
- First-Coat Seal (Single-Coat Seal), 180/200 pen. grade, 3 pph Kerosene, 0.7 pph Adhesion Agent, Grade 4 SC12 chip ALD 7.77 mm, Application Rate 1.50 λ/m^2 hot.
- Second-Coat Seal (Two-Coat Seal), 180/200 pen. grade, 1 pph AGO, 4 pph Kerosene, 0.7 pph Adhesion Agent, Grade 3 SC16 chip ALD 8.76 mm, Grade 5 SC10 chip ALD 5.00 mm, Application Rates 1.0 λ/m^2 first spray, 0.8 λ/m^2 second spray (both hot application rates).

3.4 Pavement Testing

For this project the SLAVE units were run in concentric offset wheel paths. Previous projects had used wide-based single tyres when the SLAVE units were run in offset wheel paths. However this project specified the use of standard dual-tyre assemblies. As the dual-tyre assembly is considerably wider than a wide-based single tyre (560 mm v 300 mm), this meant that separation between the two vehicles would not be sufficient, even with a narrow wander pattern. To overcome this limitation, a 300 mm-long extension section was fitted to arm B. Thus the radial distance between the centrelines of the vehicles was 1100 mm and the clear separation between the vehicles was 450 mm, with the vehicles operating on a ±50 mm normally distributed wander pattern.

Descriptions of testing in Tasks 1 and 2 of the 2000/2001 project are in the relevant reports (de Pont et al. 2001, Arnold et al. 2001). Details of measurement procedures and frequency for Task 3 are outlined below.

After the pavement design meeting, and considering the possible scuffing affect of the dual wheels on the surface, the decision was to change to single wheels with a corresponding reduction in static load. All other parameters were set to the same as previous tests.

For 5000 laps of surface conditioning, the vehicles ran at minimum weight (21 kN) with the single wheel mounted on the inside position on the inner vehicle and on the outside position on the outer vehicle. A loading pattern was devised to ensure an even number of passes over the entire traffickable width, applied at 10 km/h under regular inspection.

After the conditioning, the chipseal surface texture was measured by the Stationary Laser Profilometer and sand circle methods, and the hardness measurements were repeated. Temperature sensors were placed on the chipseal surface and air temperatures were also recorded, at each of the three measurement stations. Temperatures were logged at 10-minute intervals continuously for the duration of the test. Temperatures were generally very cold (less than 10°C) in the first 100 000 laps of loading but rose steeply to over 20° after that.

The outer wheel was refitted on the inside position and a loading pattern devised to replicate the dual-tyre pattern of the original tests. The previous 40 kN load on dual tyres was replaced by a 21 kN load, and the 50 kN load on dual tyres was replaced with a 26 kN load. Loading speed was reduced to 20 km/h to take into consideration the unknown effect on the surface. Loading was confined to standard working hours so the condition of the surface could be regularly monitored.

Stationary Laser Profilometer readings were taken at 1000, 2000, 3000, 4000, 5000, 7500, 10 000, 15 000, 20 000, 25 000, 30 000, 40 000, 50 000, 70 000, 100 000, 125 000, 150 000, and 175 000 passes. Rig speed was increased to 30 km/h after 15 000 laps.

At 4000 passes the tyres began to pick up bitumen and chip from the surface. New tyres were fitted and the track surface was carefully inspected for the source of the bitumen, and some minor cleanup was undertaken. Bitumen and chip on the edge of the asphalt was removed by heat gun and sand was applied. The vehicle geometry was carefully checked and was exactly to specification. At 7500 passes the asphalt concrete repair in Section C itself appeared to be the problem so an epoxy and bauxite chip overlay was applied to the asphalt.

At 25 000 cycles, tyres picked up bitumen and chip again and the effect of this can be seen in the results. A sprinkler system mounted on the rear of the vehicles was developed using a low pressure feed from a water tank, mounted on the centre of the rig, to microjets on the vehicles with the application controlled by an electronic timer and solenoid valve. The timing had to be adjusted for different air temperatures but overall the system was quite effective and allowed continued testing.

Towards the end of the project, continuous watering was required because of the higher temperatures, and an overhead supply was developed to fill the tank on the rig.

During the project the tyres had to be cleaned three times and replaced three times because of a thin build-up of bitumen on the tyres. The two-coat application of the Grade 3 & 5 seals possibly aggravated the situation, and a racked-in application should be used in future.

After the vehicle tyres had stuck to the surface while stationary, then ripped up sections of the seal once moving again, removable steel plates were laid down where the vehicles had to be stopped. These sections were repaired but the water applied did get into the repair joints and caused localised minor basecourse movement near the end of the project.

At 175 000 passes, the surface texture had reduced to the point where the seal started to bleed, and so the test was halted. At this time, final Stationary Laser Profilometer testing was undertaken and sand circles were repeated. Sections of seal across both wheel paths were cut out, measured, and photographed. Samples of bitumen that had adhered to the tyres were recovered for laboratory testing.

4. Results & Analysis

4.1 Introduction

As noted in Section 1.1, the main concern of this study is pavement wear as represented by a loss of functional condition. For the thin-surfaced unbound granular pavements that predominate on New Zealand roads, the main aspects of functional condition that lead to the need for maintenance and rehabilitation are roughness, rutting, cracking, and loss of skid resistance. Vertical Surface Deformation (VSD) reflects the roughness and rutting changes, while surface texture changes are an indicator of a loss of skid resistance.

Consequently, the effect of mass on the pavement surfacing, and in particular on surface texture, is the primary concern of this Stage 2 of the study. However, because surface texture v loading cycles history has similarities to the VSD v loading cycles history, which was analysed in Stage 1 of this project (reported by de Pont et al. 2001), the VSD results are re-visited and the models of the two forms of pavement distress are compared. Section 4.3 considers the surface texture changes and the effect of mass on these (see Appendix for the data records); Section 4.4 re-visits the VSD data and the Compaction-Wear model derived in the previous report; and finally Section 4.5 compares the two types of wear.

4.2 Impact of Higher Mass Heavy Vehicles on Wear of Existing Pavements

The first task of the 2000/2001 research was to measure the response of the pavement to a matrix of tyre type, inflation pressure, speed and load. This work was funded by AUSTROADS and the data has been analysed and reported by ARRB Transport Research Ltd[3] (Vuong & Sharp 2001). During testing by AUSTROADS 19 000 load cycles were applied to the pavement. Because of the high loading levels in some tests (up to 60 kN on wide-based single tyres), a measurable increase in the VSD was recorded during the duration of this testing. The increase in VSD is shown in Table 4.1. As can be seen in the table, the changes were quite high, compared to the measured level of VSD after 1 000 000 load applications.

Table 4.1 Increase in average VSD during Stage 2, Task 1 testing.

Section	Average VSD (mm) at 1 000 000 load cycles	Average increase in VSD (mm) after AUSTROADS tests, at 1 019 000 load cycles
A	6.0	1.3
B	6.5	0.7
C	4.5	0.9
D	4.2	1.2

[3] Australian Road Research Board Transport Research Ltd, Vermont South, Victoria, Australia.

After 1 000 000 load cycles from the 1999/2000 research project, and the 19 000 cycles from Task 1 of the 2000/2001 research, the effect of increasing the vehicle mass on a pavement structure that had already been trafficked by a lower vehicle mass was investigated in Task 2.

For this Task 2, the axle load was increased to 10 tonnes and 300 000 load applications were applied. The outer wheel path was trafficked by a 6.0-tonne axle load so that the level of distress of the pavement would not increase. The condition of the outer wheel path was not monitored for this work. The average inner wheel path VSD for each pavement segment is shown in Figure 4.1. This figure shows a rapid increase in the VSD immediately after the increase in load, and then the rate of VSD increase is similar to the rate for the first million laps.

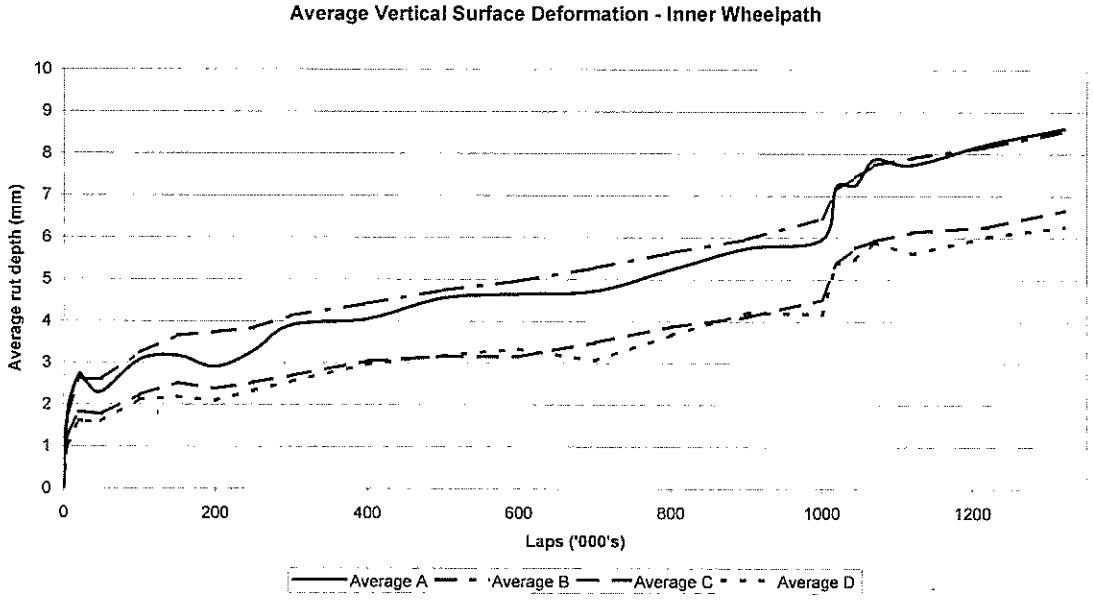

Figure 4.1 Average VSD for each segment in the inner wheel path after 1 320 000 load cycle applications.

The VSD data from 1 000 000 to 1 320 000 laps have been analysed using the "Compaction-Wear" model proposed in Stage 1 of this work. An offset has been applied to data with respect to the total VSD and total number of laps so that at 1 000 000 laps the data has a VSD of 0 mm and a lap count of zero.

The Compaction-Wear model was applied in three different ways. The first method applied the 10-tonne equations to the data, but the initial compaction factors (i.e. intercept of the wear line) were much higher than the total amount of VSD. The results of this are shown in Figure 4.2.

The second method also applied the 10-tonne equations to the data but in this case the compaction factors were set to be equal to the difference between the 8-tonne and 10-tonne compaction factors. This approach, while giving a better fit to the measured data, was still not satisfactory. The results are shown in Figure 4.3.

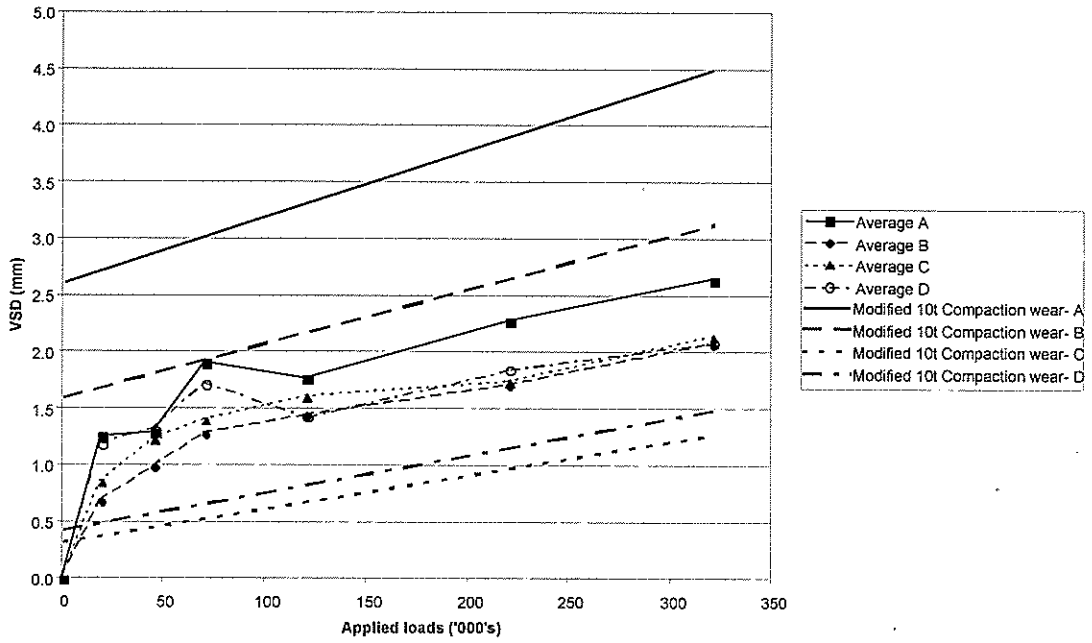

Figure 4.2 VSD data fitted with original 10-tonne Compaction-Wear model.

Figure 4.3 VSD data fitted with modified 10-tonne Compaction-Wear model.

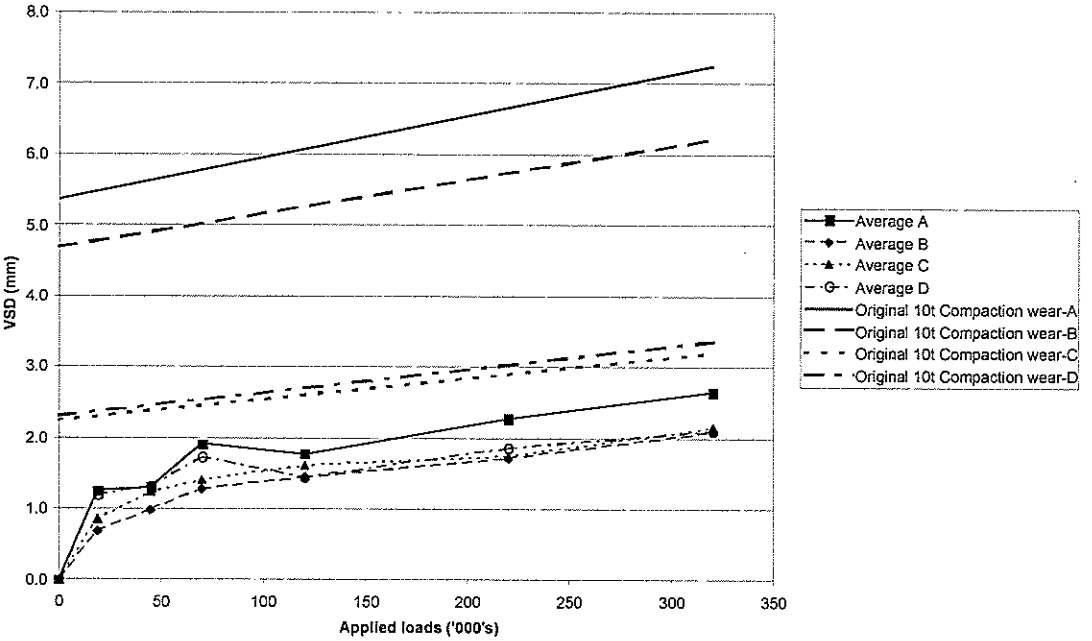

The third method was to develop new coefficients for the Compaction-Wear model. For this approach, the data from 70 000 to 320 000 was used to determine the slope and intercept values. The new coefficients are shown in Table 4.2. If the slope coefficients are compared with the slope coefficients determined for the previous (8-tonne and 10-tonne) models, the coefficients for this data set are shown to be closer to the coefficients for the 8-tonne data (Table 4.3), except for Segment C which had been modified.

The rate of increase of the VSD would be expected to be similar to that of the 10-tonne (outer wheel path) axle load measured in Stage 1 of this work, as it was the same pavement. However the results show that the VSD rate is closer to that measured under the 8-tonne axle load, although the current set of data was measured on the original 8-tonne wheel path. The implication of this finding is that existing pavements may show an initial increase in roughness type of deterioration when subjected to an increase in axle loads, but the long-term rate of deterioration may not be all that different from the present deterioration rate. It is difficult to determine the effect related to the mix of loading conditions used in Stage 2, Task 1 of this project, especially with respect to the initial changes that occurred straight after the increase in axle load.

Table 4.2 Linear fit parameters for VSD v load cycles on inner wheel path.

Segment	Intercept - Compaction (mm)	Slope – Wear rate (mm/1000 load cycles)	Goodness of fit - R^2
A	7.50	0.00335	0.899
B	7.52	0.00313	0.996
C	5.75	0.00274	0.958
D	5.59	0.00200	0.654

Table 4.3 Comparison of the slope coefficients for the different data sets.

Segment	Previous model		Current data
	8 tonne	10 tonne	10 tonne
A	0.00321	0.00586	0.00335
B	0.00327	0.00480	0.00313
C	0.00245	0.00299	0.00274
D	0.00233	0.00332	0.00200

4.3 Impact of Higher Mass Heavy Vehicles on Surface Texture Changes

The traditional method for measuring surface texture is the volumetric patch technique using sand or glass spheres (sand circle method). This technique, although very simple, is quite labour intensive and time consuming. There is also a degree of technician-dependent variation in the results. As an alternative the International Standards Organisation (ISO 1997) has developed a procedure using the surface profiles, and this gives comparable results.

This enables use of laser and other profilometers to make the measurements, with mathematical processing of the results to obtain texture depth measurements. By specifying the performance requirements of the profilometer and the measurement procedure in detail, this approach ensures standards of accuracy and repeatability. Because the profilometer measurement process can be automated and can be undertaken at relatively high speeds compared to the sand circle method, texture measurements can be done quite rapidly and at frequent intervals along the pavement.

With the ISO method, the profile is measured along a baseline which is 100 mm ± 10 mm long. The baseline is divided in half and the peak level of the profile in each half is determined. These two values are then averaged to give the profile peak, and the Mean Profile Depth (MPD) is defined as the profile peak minus the average profile level. From the MPD, a parameter known as the Estimated Texture Depth (ETD) can be calculated using Equation 1:

$$ETD = 0.2 + 0.8 \cdot MPD \qquad \text{Equation 1}$$

ETD is an estimate of the Mean Texture Depth (MTD), which is the measure generated by the volumetric method. It is calculated by dividing the volume of sand used by the area of the circle created. Details of the specific measurement and processing requirements for determining MPD are given in the ISO standard (ISO 1997).

The laser profilometer at CAPTIF was used to determine MPD in each of the two wheel paths around the track. Readings were averaged over a length of 1655 mm centred at every second measurement station. At the start of the test, 1000 load cycles were applied between measurements, but this was gradually increased as the test proceeded so that, by the end of the test, 25 000 load cycles were applied between measurements. Plotting the progression of MPD against load cycles for each station showed a high degree of variation and any clear trends were difficult to see. However, averaging the MPD for the whole circuit in each wheel path and plotting against load cycles did show a clear trend, and shows that the two wheel paths are different as illustrated in Figure 4.4.

The interesting features to note in this figure are:

- First, the plot began at 5000 load cycles. This was because 5000 conditioning laps were applied after the chipseal was placed. These loads were applied by making both vehicles traverse evenly the full traffickable width of the track. Thus, both wheel paths should have received the same applied loads. However, the initial average MPD for the two wheel paths was not identical. It is believed that this was caused by uneven spreading of the stone chips in the radial direction because of the circular track.
- At two measurement sets early in the test (9000 and 25 000 loads), the MPD increased and it did so in both wheel paths by a similar amount. This occurred because high surface temperatures caused the bitumen to soften sufficiently for the tyres to pick up stones from the surface. This form of surface wear is called

"ravelling". Although this represented a loss of condition for the pavement, the short-term effect was to increase the mean texture depth and hence improve the MPD.

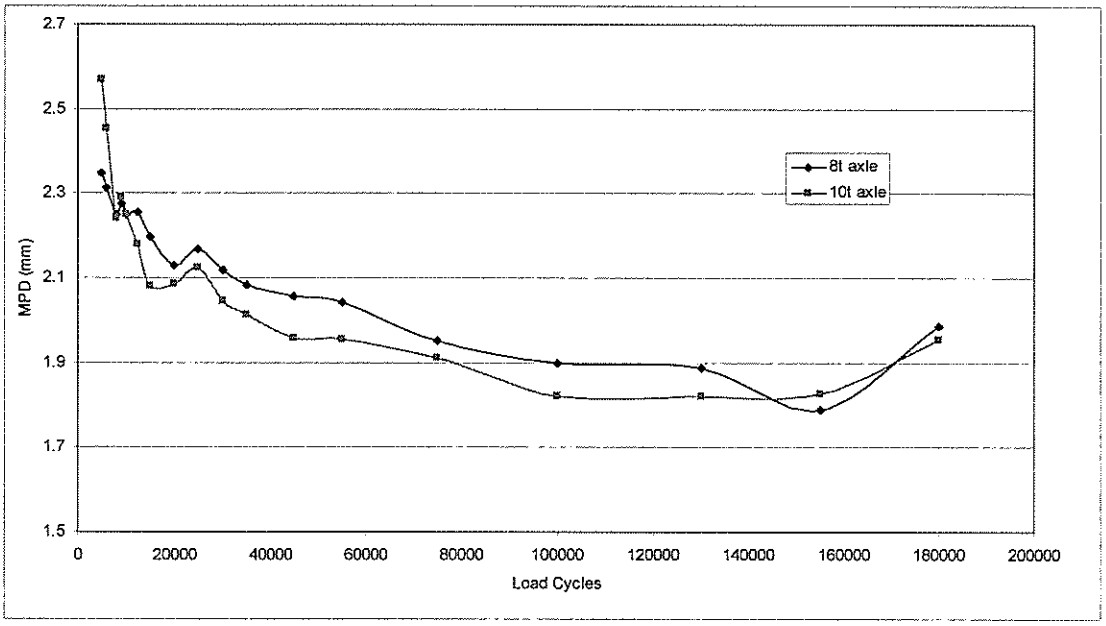

Figure 4.4 Average MPD for each wheel path against applied load cycles.

- Similarly at the end of the test, the MPD on both wheel paths was increasing noticeably. At this point the bitumen had bled over the stone chips and stuck to the tyres. Because bitumen had been removed from the surface, again this gave the impression that the pavement condition was improving.

These last two points highlight the fact that MPD is merely an indicator of surface condition and needs to be interpreted in conjunction with visual observations in order to accurately assess the condition of the surface. Both ravelling and bleeding were observed visually.

4.3.1 Patrick and Cenek Models

Transit New Zealand (1998) presents the following model for texture depth, which was developed by Patrick for Transit NZ Specification P17, based on the work by Houghton & Hallett (1987).

$$TD = k - ALD \,.\, B \,.\, \log T \qquad \text{Equation 2}$$

where
- TD is the texture depth
- k is a constant which depends on ALD and the bitumen spray rate
- ALD is the average least dimension of the sealing chip
- B is a constant
- T is the total traffic to date in equivalent light vehicles where one heavy vehicle is equivalent to 10 light vehicles

Cenek (1999) derived the following incremental model for texture depth from the Patrick model.

$$\Delta TD = k_1 - TD - k_1.k_2.\log\left[10^{\left(\frac{1}{k_2}\frac{TD}{k_1.k_2}\right)} + \Delta NELV\right]$$ Equation 3

where ΔTD is the change in texture depth

$\Delta NELV$ is the number of equivalent light vehicles over the time period

k_1 is the initial texture depth after construction

k_2 is the rate of change of texture depth with traffic

Showing that the two models are identical is relatively straightforward, where $k_1 = k$ and $k_1.k_2 = ALD.B$. Note that this model is based on curve fitting to the measured data and does not represent a postulated wear mechanism. Both Patrick (Transit NZ 1998) and Cenek (1999) calculated estimates for the coefficient values based on observed data.

Patrick obtained a value of B = 0.07. He did not present values for k because the model is used to look at changes in MPD and thus the k can be eliminated from the equation. Cenek (1999) however presents a table of values for k_1 and k_2, where k_1 depends on both the chip grade and the design traffic, while k_2 depends only on the chip grade.

As the bitumen spray rate depends on the design traffic, the dependencies of k_1 in Cenek's model are the same as those of k in Patrick's model. For Grade 3 chip with ALD = 9.5 mm, the k_1 and k_2 values given by Cenek result in B values between 0.078 and 0.092 depending on the design traffic volume. For Grade 5 chip with ALD = 4.5 mm, the k_1 and k_2 values given by Cenek result in B values between 0.091 and 0.107 depending on the design traffic volume. In all cases, a higher design traffic value implies a higher B coefficient and, also in all cases, the B coefficient is greater than the value given by Patrick.

Although the Patrick and Cenek models represent a statistical fit to observed data rather than a mechanistic model, investigating the implications of the model is worthwhile before attempting to fit it to the current data. The Patrick form of the model is somewhat simpler and easier to work with. Basically the equation can be written as:

$$TD = c_1 - c_2.\log T$$ Equation 4

where c_1 and c_2 are constants which depend on the pavement design.

Differentiating this equation gives:

$$\frac{dTD}{dT} = \frac{-c_2}{2.3026\ .T}$$ Equation 5

From these two equations, a number of properties of the model can be deduced. Because of the properties of the log function, the model does not behave well when T is less than one. The texture depth at construction (after one equivalent light vehicle) is c_1 (mm). Similarly the rate of change of texture depth with traffic at construction is $-c_2$ (mm)/equivalent light vehicle. The rate of change of texture depth with traffic

subsequently is inversely proportional to the total amount of traffic that has passed. Thus the rate of change reduces very quickly initially and asymptotes to zero.

Now consider how the model might be applied to the test data. The calculation of the traffic in equivalent light vehicles assumes that each heavy vehicle is equal to ten light vehicles. However, how many light vehicles a single pass of an 8-tonne or a 10-tonne axle is equal to is not clear. If each pass of an 8-tonne axle is assumed to be equal to α equivalent light vehicles, and each pass of a 10-tonne axle is assumed as equal to β equivalent light vehicles, then if the ratio of β to α can be determined, the relative effect of mass on texture depth changes has been determined. Substituting for the simplified Patrick model (Equation 4) gives:

$$TD_{8t} = c_1 - c_2 . log\alpha N$$
$$= c_1 - c_2 . log\alpha - c_2 . logN \qquad \text{Equation 6}$$

Similarly

$$TD_{10t} = c_1 - c_2 . log\beta - c_2 . logN$$

where: N is the number of load cycles

The effect of the increase in mass is to change the initial texture after one pass of the axle by c_2.log(α) for the 8-tonne axle and by c_2.log(β) for the 10-tonne axle. Otherwise there is no difference in the equations. As c_1 and c_2 are properties of the pavement only and should be identical in both wheel paths, one equation is subtracted from the other to give:

$$TD_{10t} - TD_{8t} = c_2 . \log\left(\frac{\alpha}{\beta}\right) \qquad \text{Equation 7}$$

This implies that the difference in texture depth between the wheel paths will be constant as the number of load cycles changes. In the model the only effect of an increase in mass is a one-off reduction in texture depth. From then on the rate of change in texture depth is exactly the same as it was at the lower mass. Intuitively this seems unlikely to be the case in practice but it is what the model implies.

Substituting from Equation 1, Equations 6 and 7 can be re-written in terms of MPD as follows:

$$MPD_{8t} = 1.25 . c_1 - 0.25 - 1.25 . c_2 \log\alpha - 1.25 . c_2 \log N \qquad \text{Equation 8}$$

and $$MPD_{10t} = 1.25 . c_1 - 0.25 - 1.25 . c_2 \log\beta - 1.25 . c_2 \log N$$

$$MPD_{10t} - MPD_{8t} = 1.25 . c_2 \log\left(\frac{\alpha}{\beta}\right) \qquad \text{Equation 9}$$

4.3.1.1 *Best fits for Patrick and Cenek models*

Applying log function fits of the modified form of the Patrick model as shown in Equation 8 gives the graphs shown in Figure 4.5. Note that the final measurement point in each trace (after bleeding has occurred) was removed before the fitting was

done. The quality of the curve fits as indicated by the R^2 statistic is shown on the figure and is very good for the 8-tonne axle and quite good for the 10-tonne axle. However, these curves are clearly not parallel to each other, which had been predicted by the model.

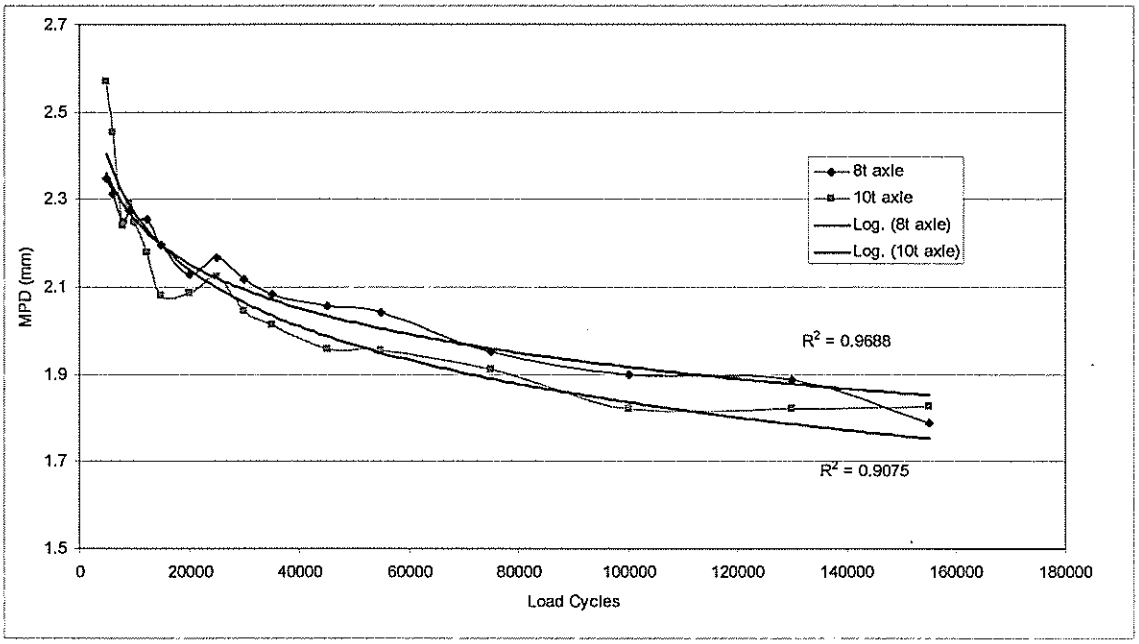

Figure 4.5 MPD v load cycles with Patrick-style log function fit for the two axle loadings (of 8 and 10 tonnes).

The equations of the best-fit curves are:

$$MPD = 3.61 - 0.3394 \log N \text{ for the 8-tonne axle, and} \qquad \text{Equation 10}$$

$$MPD = 4.02 - 0.4368 \log N \text{ for the 10-tonne axle.} \qquad \text{Equation 11}$$

Clearly the coefficient of the log N term is not the same for both equations, although the model predicts it should be. Also the constant in the 10-tonne axle equation is greater than that in the 8-tonne axle equation where it would be expected to be smaller.

Consider now the difference in MPD for the two wheel paths as shown in Figure 4.6. The Patrick and Cenek models predict that this curve should be a constant value (i.e. a horizontal straight line). The section of the curve between 15 000 load cycles and 130 000 load cycles fits this prediction to a reasonable extent although the variations are somewhat higher than desirable (mean = 0.067 mm ± s.d. 0.021 mm). Removing the end two data points from the calculation can be justified as clearly bleeding had occurred in the outer wheel path under the 10-tonne load. However, the justification for removing the first five data points is more difficult. During this early stage of the testing the texture depth is changing very rapidly and the sample points are relatively closely spaced but they do not follow the model predictions well. This indicates that the model is not a good predictor of the performance of the pavement surface during this early stage of its life. If all the data points are included in the analysis the mean difference is 0.023 mm.

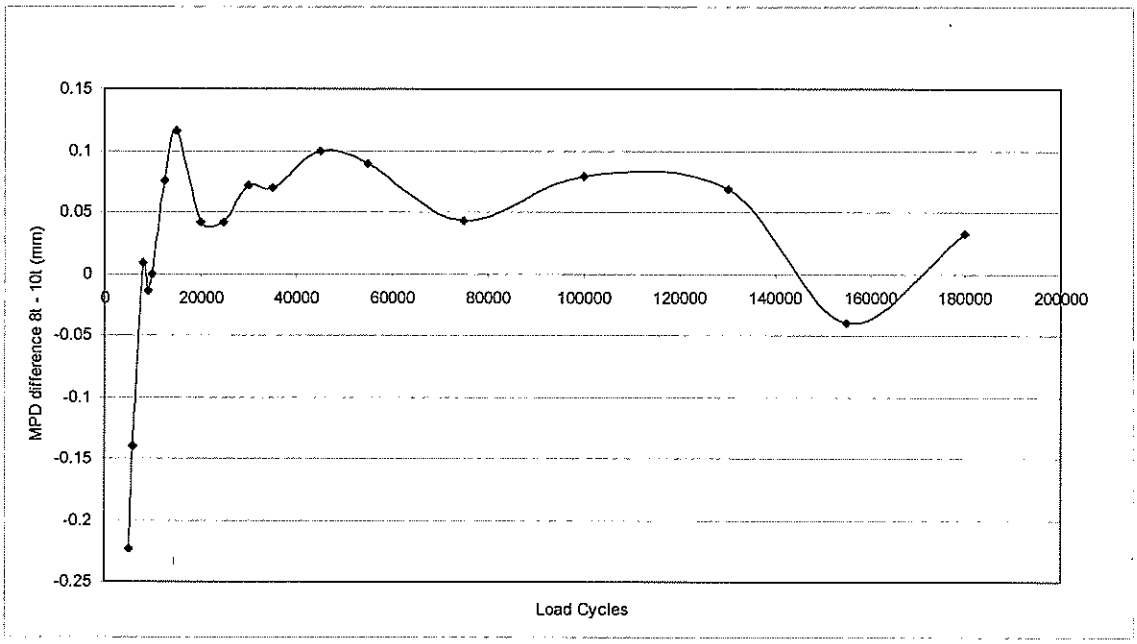

Figure 4.6 Difference in MPD between the wheel paths for the two axle loadings for inner (8 tonne) and outer (10 tonne) wheel paths.

If the 10-tonne axle results are shifted by the mean difference, a regression analysis can be undertaken for all the data to obtain the coefficients for the model.

If 0.023 mm is used for the shift the resulting equation is:

$$MPD = 3.8282 - 0.3882 \log N, \text{ which has an } R^2 = 0.92 \qquad \text{Equation 12}$$

If 0.067 mm is used for the mean, the equation is:

$$MPD = 3.8501 - 0.3882 \log N, \text{ which has an } R^2 = 0.90 \qquad \text{Equation 13}$$

The two equations are very similar with slight differences in the c_1 coefficient and the same c_2 coefficient. Applying Equation 9 with a mean difference of 0.067 mm gives $\beta/\alpha = 1.49$, while using a mean difference of 0.023 mm gives $\beta/\alpha = 1.15$. The ratio of the applied loads is 10.12/8.16 = 1.24. If the relationship between mass and wear is assumed to be a power law, then the first value (1.49) gives an exponent for the power law of 1.85, while the second value (1.15) gives an exponent of 0.65.

The coefficient of the log terms in the above equations is equal to 1.25 x c_2 (Equation 8) and c_2 is equal to ALD x B in Patrick's original model (Equations 2 and 4). As the surfacing consists of two layers, i.e. Grade 3 chip followed by a Grade 5 chip, the ALD value used in the model should be that of the largest chip, i.e. 9.5 mm. On this basis the 0.3882 coefficient is equivalent to B = 0.0327 in Patrick's model. This is just under half the 0.07 figure he uses.

4.3.1.2 *Power law fit for Patrick and Cenek models*

Assuming that one pass of the 8-tonne axle corresponds to ten equivalent light vehicles, the number of equivalent light vehicles for one pass of the 10-tonne axle can be determined for any power law exponent. The results of doing this for three

possible exponent values, 0.65, 1 and 1.85, are shown in Figure 4.7. This figure clearly shows that, of the three values, the power law with an exponent of 1.85 gives the best fit. Although in generating this figure the assumption was that one pass of the 8-tonne axle is equivalent to ten light vehicles, this assumption has no effect on which power exponent provides the best fit. If an alternative value were used, the scaling of the x axis in the figure would change but the traces would all retain the same shapes and relative positions to each other.

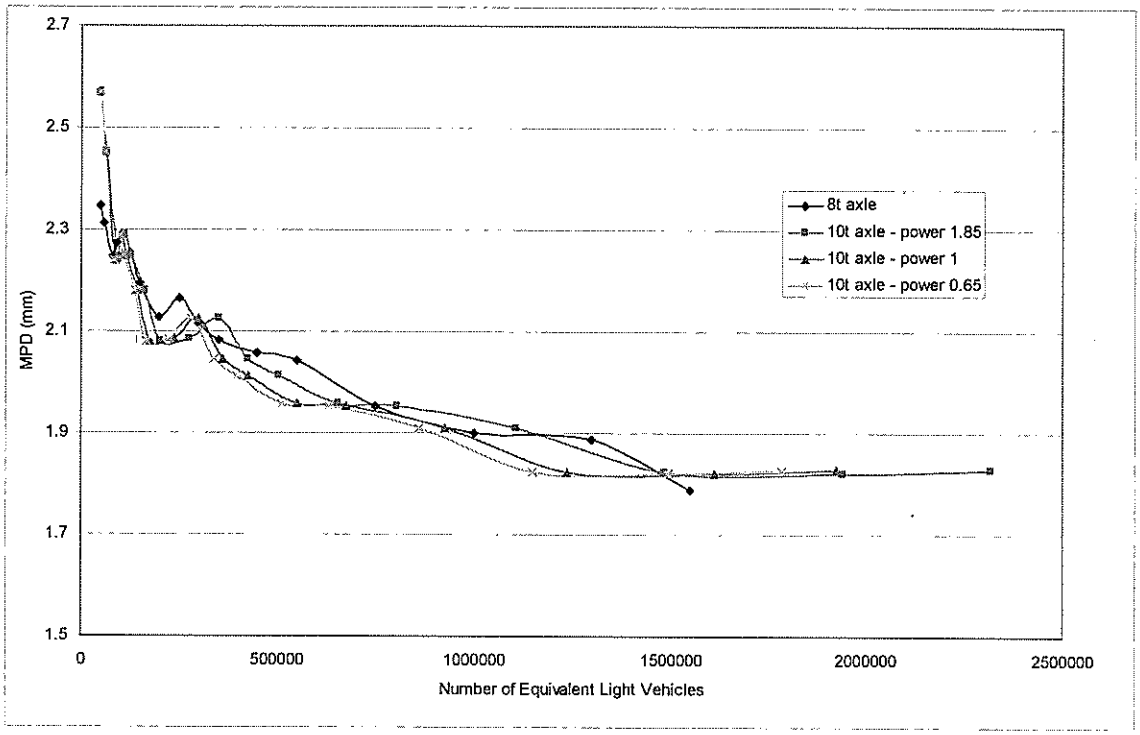

Figure 4.7 Power law fits (of 1.85, 1, 0.65) to MPD loss for the two axle loadings (8 and 10 tonnes).

The power law model predicts the relative wear contribution from different axle loads. It does not model the damage from repeated load cycles of a single axle mass such as the 8.2-tonne axle used for this study at CAPTIF. This is done with a model like the Patrick and Cenek models described above. For VSD which was considered in Stage 1 of this project (de Pont et al. 2001) a Compaction-Wear model was developed.

This model postulated two components to the pavement deterioration: an initial phase called *compaction* which occurs immediately after construction that involves a rapid change in VSD, and a phase called *wear* where VSD increases steadily with increasing load cycles. This wear phase was approximately linear, and so the model was fitted by applying a linear regression to the measured data from this phase.

The progression of MPD with loads appears at first glance to have similar characteristics to the VSD progression with an initial rapid change followed by a slower steady change. (The changes are, of course, in the opposite direction because increasing VSD implies deterioration while decreasing MPD implies deterioration.)

Applying a linear regression fit to the data between 15 000 load cycles and 100 000 load cycles gives good results (R^2 = 0.96 for the 8-tonne axle data and R^2 = 0.92 for the 10-tonne axle data). However, including the data from the next data points (at 135 000 load cycles) degrades these fits (R^2 = 0.92 for the 8-tonne axle data and R^2 = 0.89 for the 10-tonne axle data) noticeably. The log fit as used by the Patrick model is much better (R^2 = 0.96 for the 8-tonne axle data and R^2 = 0.91 for the 10-tonne axle data). This suggests that the linear wear model used for VSD is not as good as the logarithmic Patrick model.

4.3.2 Kinder-Lay Model

Kinder & Lay (1988) developed a model to describe the progression of permanent deformation with loads. This model has the form:

$$VSD = KP^m N^{\frac{m}{\alpha}} \qquad \text{Equation 14}$$

where K, m and α are constants
P is the axle load in tonnes
N is the number of load cycles

It takes into account both a power law for the effect of mass, and the rate of change of VSD changes as load cycles increase. It also shows that α is the exponent of the power law. With surface deformation the model goes through the origin, i.e. at zero load cycles there is zero deformation. Applying a similar form of model to MPD requires a minor modification to the model to take into account that, at zero load cycles, the MPD is not zero. A suitable form of the model is:

$$MPD = MPD_0 - KP^m N^{\frac{m}{\alpha}} \qquad \text{Equation 15}$$

where MPD_0 is the mean profile depth in mm at zero loads

From the test, data are available for two different levels of load. Applying the model to each load magnitude and combining the two equations we get:

$$MPD_2 = MPD_0\left[1 - \left(\frac{P_2}{P_1}\right)^m\right] + MPD_1\left(\frac{P_2}{P_1}\right)^m \qquad \text{Equation 16}$$

where the subscripts 1 and 2 denote the two load cases

Applying linear regression to this equation, best fit estimates are obtained for MPD_0 and m. Alternatively Equation 15 can be rewritten as:

$$\frac{MPD_0 - MPD}{P^m} = K.N^{\frac{m}{\alpha}} \qquad \text{Equation 17}$$

Substituting MPD_0 and m, we can take logarithms and use linear regression with the data from both loads to obtain best fit estimates of K and α. The best estimates of the parameters and the R^2 statistic obtained by applying the above process to the measured data between 8000 load cycles and 130 000 load cycles, are shown in Table 4.4.

Table 4.4 Best estimates of parameters in Kinder-Lay style model.

MPD_0	m	α	K	R^2
2.5422	0.5722	1.6896	0.003867	0.95

This model is only slightly better than the Patrick model (higher R^2 value) but it has the advantage for this study as it explicitly includes the effect of mass. As explained above, the parameter α is the exponent of the power law relationship for the effect of mass. This model estimates 1.69 for α, which is very similar to the 1.85 value derived by applying the Patrick model.

Figure 4.8 shows a comparison of the Kinder-Lay style model with the measured data for each of the wheel paths. The fit for the 8-tonne axle load is clearly better than that of the 10-tonne axle load, where the match at the beginning and end of the test is not so good. The situation at the end of the test (last two measurements) is understandable as the surfacing had failed, and the tyres were removing the bitumen. However, it is not clear why the actual MPD on the 10-tonne outer wheel path after 5000 conditioning laps should be so much higher than the value on the 8-tonne inner wheel path. Possibly the circular nature of the track may have caused the thickness of chips on the inner wheel path at construction to be greater than on the outer.

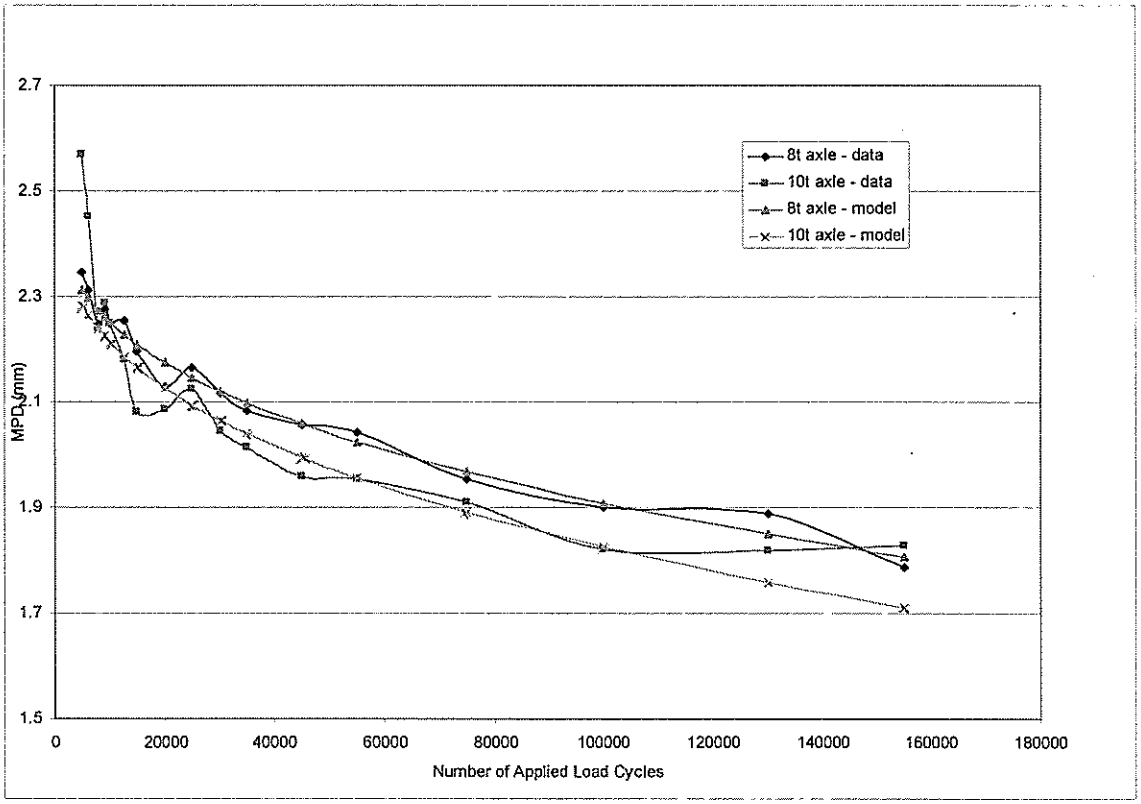

Figure 4.8 Comparison of MPD predicted by Kinder-Lay style model with measured data for two axle loadings (8 and 10 tonnes).

4.4 Review of Vertical Surface Deformations (VSD)

4.4.1 General Power Law Relationship

In the original 1999/2000 project (de Pont et al. 2001), the change in VSD for each of the four pavement segments was analysed. The first model fitted to the data was a power law model of the form:

$$\frac{N_{inner}}{N_{outer}} = \left[\frac{P_{outer}}{P_{inner}}\right]^n \qquad \text{Equation 18}$$

where n is the exponent of the power law

N is the number of applied load cycles to reach a level of VSD

P is the axle load

Three methods were used to create the dataset for estimating the best fit value of n:

1. For every measured value of VSD and load cycles on the inner wheel path, the number of load cycles on the outer wheel path to generate the same VSD were calculated by interpolation.
2. The number of load cycles on the inner wheel path needed to generate the measured VSDs in the outer wheel path were calculated.
3. The data from both the previous methods were combined.

In all three methods, because P_{inner} and P_{outer} are known, the value of the exponent n required to get the power law relationship to hold can be calculated for each VSD value. These estimates can then be averaged. Whichever of the three datasets is used makes relatively little difference to the results. Table 4.5 summarises these results.

Table 4.5 Best fit exponent values for general power law model, using the three methods.

Segment	Method 1	Method 2	Method 3
A	8.9	9.3	9.0
B	6.1	6.3	6.2
C	2.8	2.9	2.8
D	3.8	3.9	3.8

Although using these values in a model gives a reasonably good fit to the measured data, the large variation in exponent values between relatively similar pavements is a major problem. For this model to be useful as a predictive tool, it is essential to be able to set an exponent value in advance. This is the principle behind the fourth power law which is widely used in pavement design and pavement management.

Using the power law relationship, the number of load cycles of the 10-tonne axle load can be converted to an equivalent number of load cycles of a standard 8.2-tonne axle load. Plotting VSD against equivalent load cycles should give similar curves for the inner and outer wheel paths.

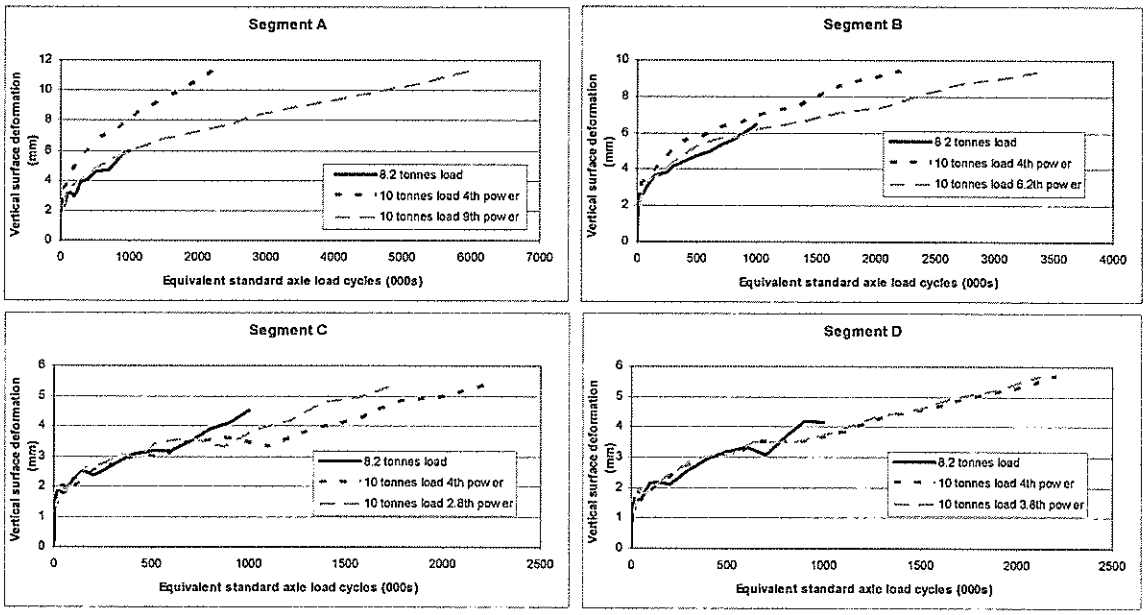

Figure 4.9 Comparison of best-fit exponents (for each segment), with the fourth power law model, for 8.2-tonne and 10-tonne wheel loads.

Figure 4.9 shows a comparison of the inner and outer wheel VSDs against equivalent load cycles for the best fit exponent and for the fourth power law. As expected, in all cases the best fit exponent model gives a reasonably good match which is better than the fourth power model. For Segments A and B the fourth power model is poor, for Segment C it is fair, while for Segment D it is quite good.

4.4.2 Kinder-Lay Model

The power law model explains the relative effect of load but does not describe the underlying shape of the VSD against load cycles curve. The Kinder-Lay form of model given by Equation 14 incorporates both a power law relationship for the effect of mass and a description of the VSD against load cycles relationship. By taking logarithms and using least squares regression, a best fit Kinder-Lay model can be developed for each pavement segment. The best fit parameters are listed in Table 4.5. As shown above, α in the Kinder-Lay model corresponds to the exponent in the power law and the values of α in Table 4.6 are similar to the best fit power law exponents given in Table 4.5. The reason they are not identical is that the Kinder-Lay model also fits a power relationship to the VSD v load cycles curve which is the same for both the 8.2-tonne and the 10-tonne axle loads.

Table 4.6 Coefficients of best-fit Kinder-Lay model.

Segment	K	M	α
A	0.00063	2.607	9.98
B	0.00532	1.668	6.55
C	0.03741	0.677	2.90
D	0.00910	1.123	4.21

Figure 4.10 Comparison of a Kinder–Lay type model with measured data for the two axle loads (8 and 10 tonnes).

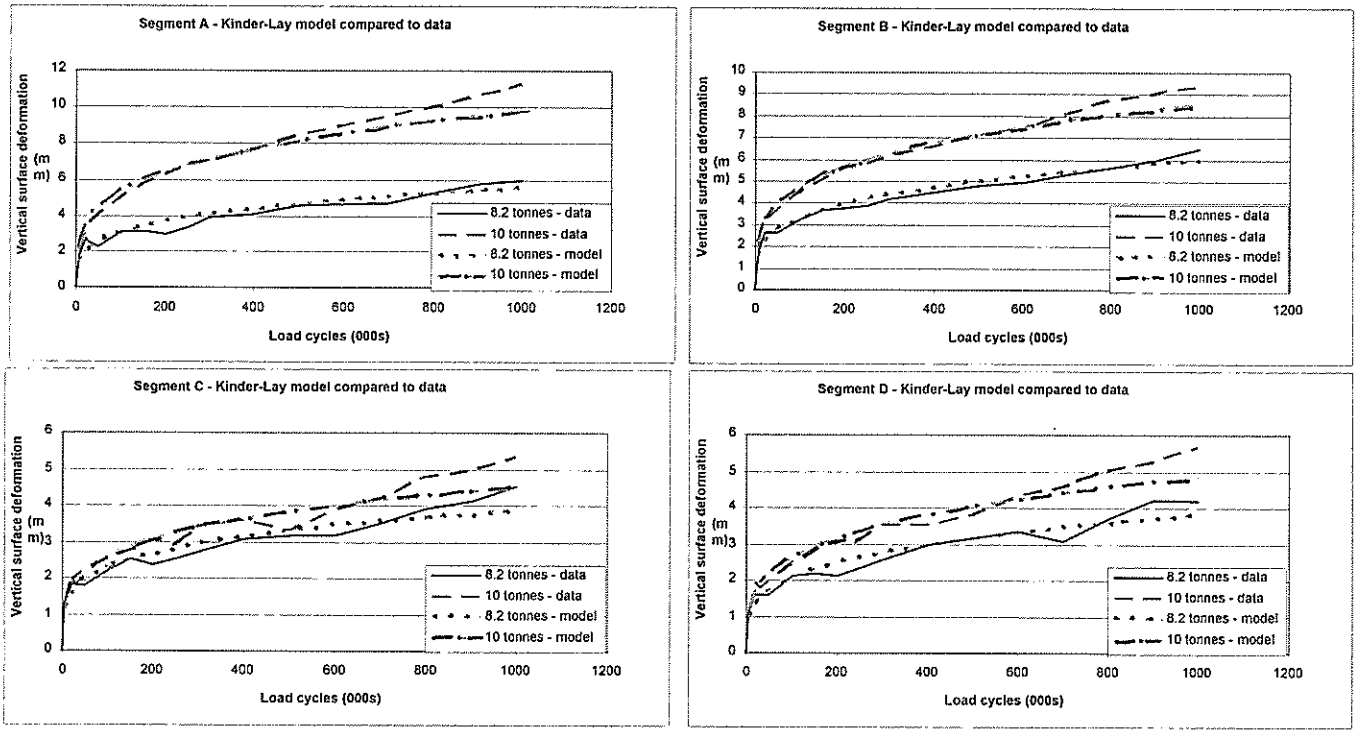

Figure 4.11 Comparison of a single Kinder–Lay type model with measured data for the two axle loads (8 and 10 tonnes).

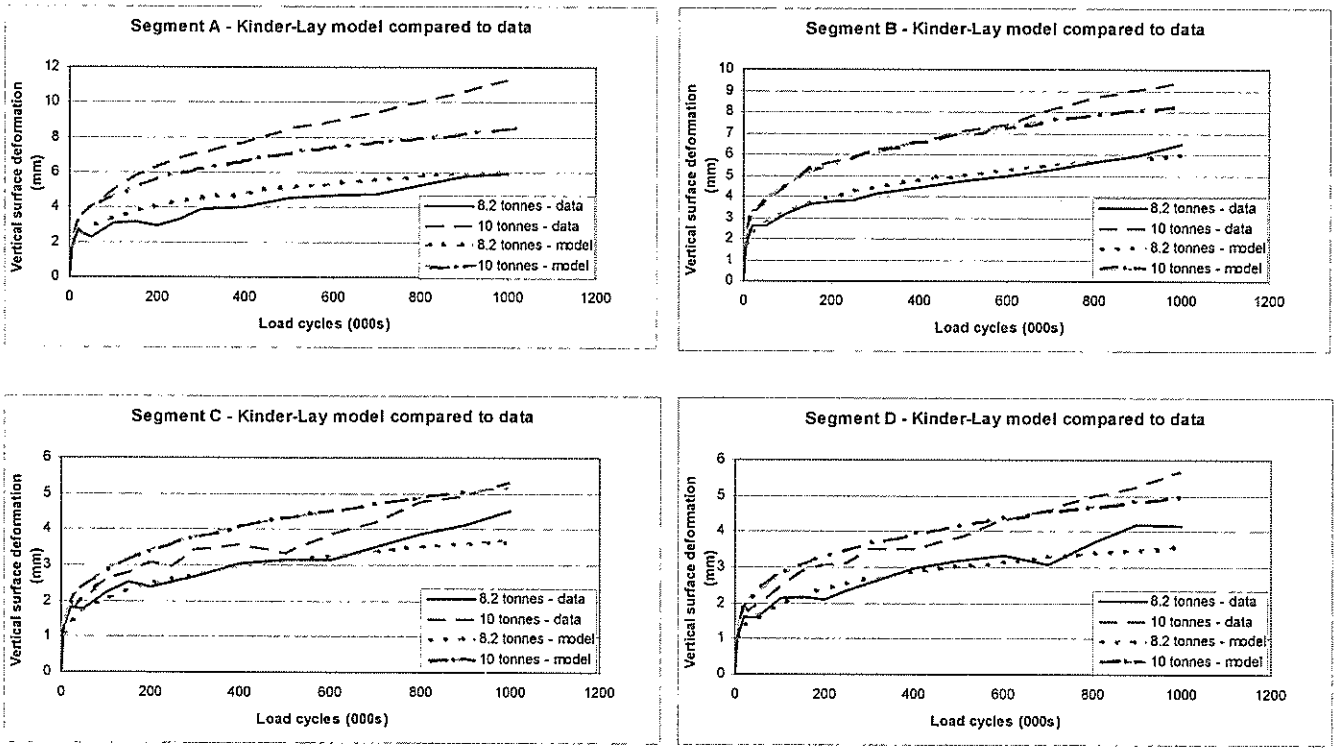

Figure 4.10 shows a comparison of the VSD v load cycle curves predicted by these Kinder-Lay type models with the measured data. As shown the fit is quite good. However, these models suffer from exactly the same problem as the power law fits shown in Figure 4.9, namely that, although the four pavement segments are quite similar, the best-fit coefficients are radically different from each other. Thus the model cannot be used as a predictive tool because the coefficients cannot easily be determined in advance. Ideally m and α should be the same for all similar pavements, and K should be pavement-specific and relate to its underlying wear resistance.

By using Segment A as the reference level and dividing the VSD values for each of the other three segments by the Segment A value at each measurement point, a best estimate of K for each pavement segment relative to K for Segment A can be determined. Adjusting the data for these K values, we can then find least squares estimates of m and α for the whole dataset and K for Segment A.

Table 4.7 Coefficients of a single best-fit Kinder-Lay model.

Segment	K	M	α
A	0.0075	1.52	5.98
B	0.0074	1.52	5.98
C	0.0046	1.52	5.98
D	0.0044	1.52	5.98

This Kinder-Lay model is suitable for predictive purposes with a single m and α (in power law terms the exponent for the mass effect is 5.98, i.e. approx. 6, Table 4.7). The K values represent the propensity of the pavement to VSD with a higher value indicating greater VSD for the same load. Thus Segments A and B are similar and more prone to VSD than C and D, which are also similar to each other. Figure 4.11 shows a comparison of the predictions of this single Kinder-Lay model with the measured data for each of the four pavement segments.

This model produces a good match for Segment B, a reasonable match for Segment D, and poorer matches for Segment C and particularly Segment A. Thus although this model has a usable form it does not provide a good fit for all four pavement segments. Note that a number of locations in Segment C were repaired during the test and thus could not be used for the analysis. Because of this, Segment C results are based on relatively few measurement stations and a poor fit for this segment is not necessarily a problem.

4.4.3 Compaction-Wear Model

In the report on Stage 1 of the project (de Pont et al. 2001), a Compaction-Wear model for the progression of VSD was developed. This model postulates that the increase in VSD consists of two components: a compaction component which occurs immediately post-construction and is largely independent of the number of load cycles applied, and a wear component which is linear with the number of applied load cycles. Stage 1 work showed that for each of the four pavement segments a power law relationship could be used to explain the effect of mass on both the

compaction and wear components. For each segment the power law exponents for compaction and wear were similar and between segments the variation was much less than for the general power law or the Kinder-Lay model as given in Figures 4.10 and 4.11. One set of coefficients for a Compaction-Wear model covering all four segments together was not developed in the Stage 1 report and this is investigated in the following discussion.

The basic form of the Compaction-Wear model is:

$$VSD = C + W.N \qquad \text{Equation 19}$$

where C is the compaction
W is the wear rate
N is the number of applied load cycles

Both C and W were shown to be proportional to a similar power of the applied load. Thus the same power exponent will be used, and a constant is needed to take account of the differences in the pavement. The full proposed model then can be written as:

$$VSD = K.P^n(C + W.N) \qquad \text{Equation 20}$$

where K is a constant reflecting the difference in VSD propensity between the pavement segments
P is the applied load
n is the exponent of the power law for the effect of mass

By comparing the VSD between the inner and outer wheel paths, the best fit value for n can be determined. Because the Compaction-Wear model focuses on fitting the linear section of the VSD against load cycles curve, only the data between 250 000 load cycles and 1 000 000 load cycles were used for estimating n. The best-fit value for n averaging across all four pavement segments is 1.82. The K value represents the relative propensity of the different pavement segments to undergo VSD. Absolute values of K cannot be determined but if one of the pavement segments is set as the reference with a K value of unity, the relative K values for the other segments can be determined in the same way as was done for the single Kinder-Lay model (Table 4.7). Dividing the VSD data from each wheel path in each segment by the appropriate K and P^n terms gives a simple linear model for all the data. Least squares linear regression can then be used to calculate C and W, and the results are summarised in Table 4.8.

Table 4.8 Coefficients of a single best-fit Compaction-Wear model.

Segment	K	n	C	W
A	1.00	1.82	0.0656	7.855E-08
B	0.98	1.82	0.0656	7.855E-08
C	0.61	1.82	0.0656	7.855E-08
D	0.59	1.82	0.0656	7.855E-08

Only the K value is specific to the pavement segment. As with the single Kinder-Lay model, K values for Segments A and B are similar as they are for Segments C and D.

4.4.3.1 *Simple Compaction-Wear model*

Figure 4.12 shows the VSD v load cycles traces predicted by the Compaction-Wear model compared to the measured data for both wheel paths in all four segments. The Compaction-Wear model assumes that the compaction occurs instantaneously at the commencement of loading and therefore does not match the initial loading cycles well.

Apart from this, the model predicts the behaviour of Segment B very well, Segment D quite well, and Segments C and A less well. However, in all cases the match is better than was achieved by the Kinder-Lay model. For Segment A, where the match is not very good, the wear rate is approximately the same as the measured data for both wheel paths and the main discrepancy is in the compaction. With the Kinder-Lay type of model the wear rate was not predicted well for Segment A.

4.4.3.2 *Blended Compaction-Wear model*

As noted in the Stage 1 report, a blending function can be used if the model is required to predict the progression of wear at the start of the pavement's life. A form of blending can be achieved if C in Equation 20 is replaced by $C.N/(N+N_0)$, where N_0 is the number of load cycles needed to achieve half the total compaction. It is clear that, as N becomes much larger than N_0, the term $N/(N+N_0)$ approaches 1 and thus the model is the same as it was without the change.

Figure 4.13 shows the Compaction-Wear model with blending (N0 = 10 000 load cycles) compared to the measured data. This blending function seems to give a good match to the measured data and has a straightforward physical interpretation.

Overall the blended Compaction-Wear model provides a better fit than the Kinder-Lay type of model. The effect of mass is accounted for by a power relationship which applies to both the compaction and the wear components in the model. For a single model encompassing all four pavement segments, the best-fit value of the exponent for this power law is 1.82, or in round numbers 2, rather than the 4 that is commonly used. However, as pointed out in the Stage 1 report, a sudden increase in mass limits will be expected to result in an increase in compaction which will occur over a relatively short time frame, as well as an increase in wear. This will give a stepped change in the VSD of the pavements which will manifest itself as increased rutting and roughness.

4.5 Discussion

For the change in texture that is indicated by MPD, the rate of change decreases with increasing load cycles. Thus a model of the form used by Kinder & Lay, which includes the number of applied loading cycles to some power, provides a better fit than the linear model implied by the Compaction-Wear model previously developed in Stage 1 of this project. For VSD, however, once the initial rapid change is completed, the rate of change is approximately constant and so the Compaction-Wear model provides a better fit.

Figure 4.12 Comparison of single Compaction-Wear model with measured data for the two loadings (8 and 10 tonnes).

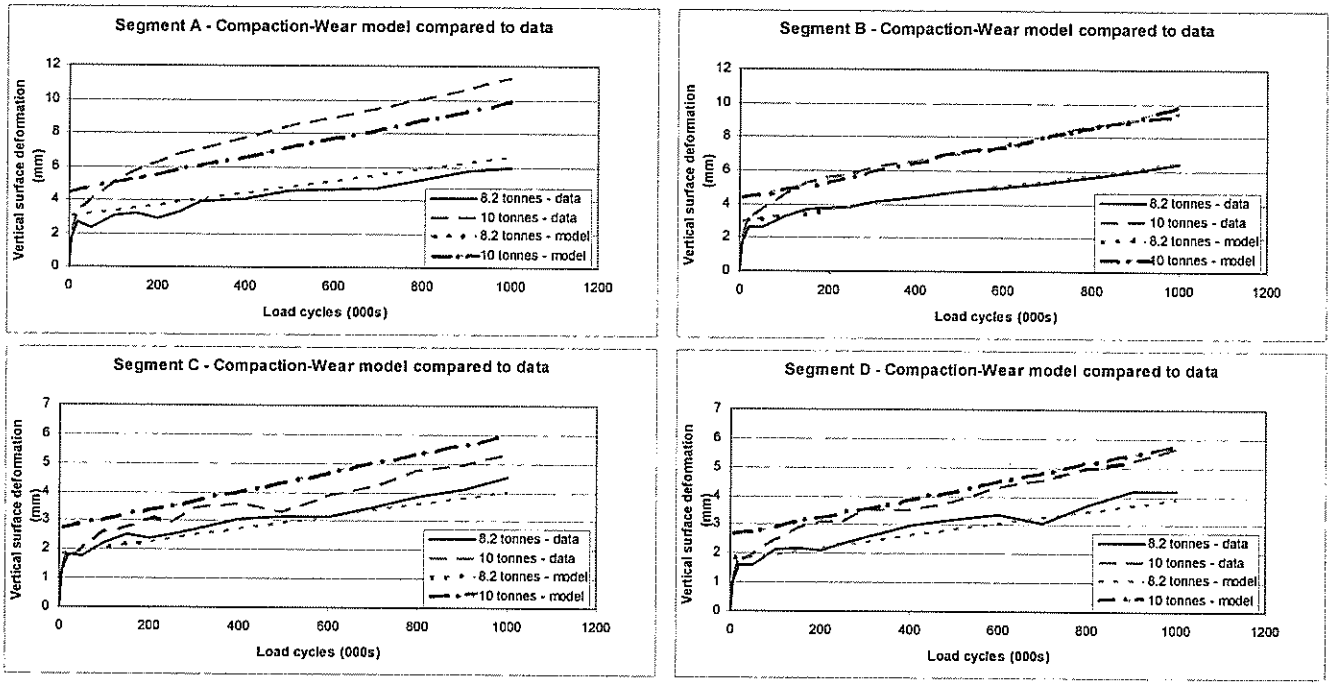

Figure 4.13 Comparison of blended Compaction-Wear model with measured data for the two loadings (8 and 10 tonnes).

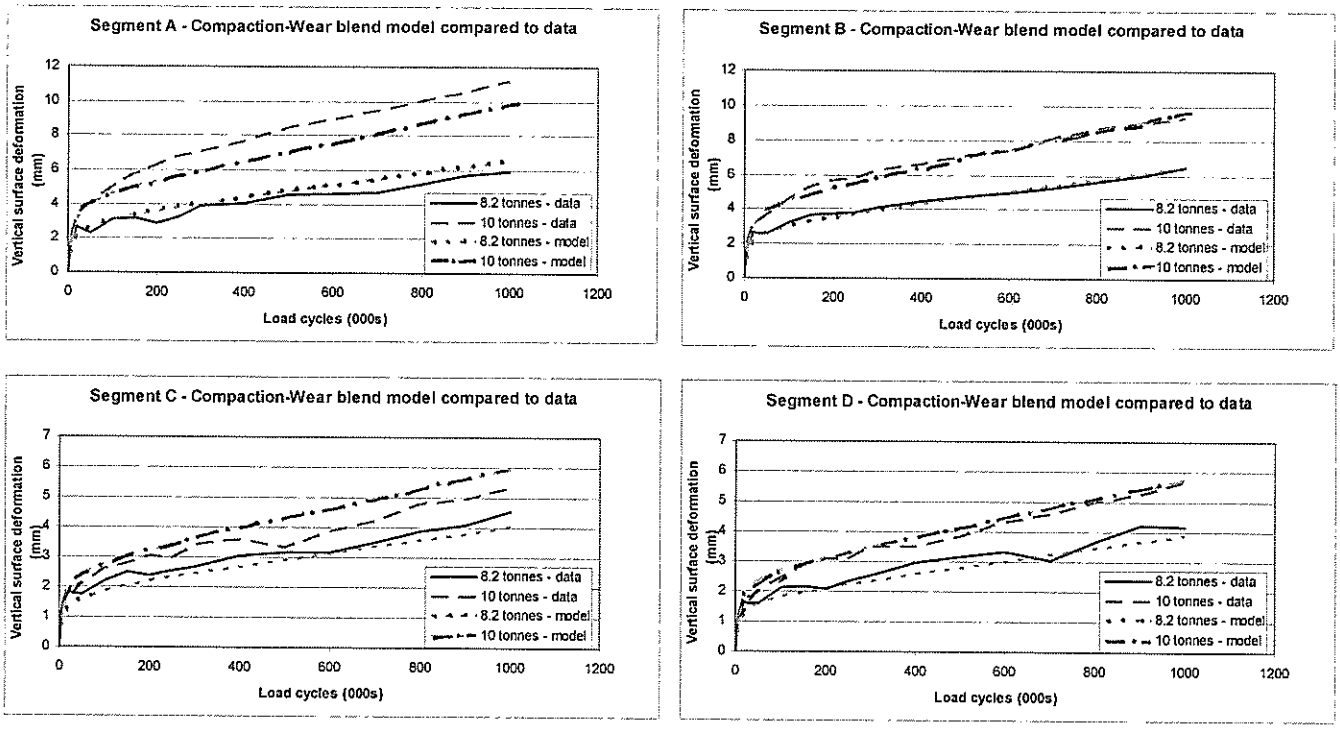

For both types of wear, the effect of mass could be accounted for by using a power law relationship. In both cases the best-fit value for the exponent of the power law was just below 2 (1.69 for texture and 1.82 for VSD, when a single model is used for all four pavement segments). For VSD, the Compaction-Wear model implies that, with an increase in mass, both an increase in compaction and an increase in wear will occur. This will manifest itself as a sudden rapid increase in VSD before stabilising to a modest increase in wear rate. The prediction was supported by measured data obtained during the tests for Stage 2 of the project.

For texture changes, the modified Kinder-Lay type of model does not predict a sudden deterioration with a change in mass limits. This does not mean it will not occur, but the model can not predict it, and no experiments have been done that specifically test this hypothesis.

5. Conclusions

The aim of this study was to compare the pavement wear generated by a 10-tonne axle load with that of a standard 8.2-tonne axle load, with a view to predicting the cost implications of a change in the legal axle load limit allowed on New Zealand's roads.

A pavement was constructed and tested at CAPTIF. It comprised four distinct segments, each of which was similar in design but utilised a different basecourse material. One of the SLAVE units at CAPTIF was configured to generate a 40 kN wheel load (equivalent to an 8.2-tonne axle) and the other was configured for a 50 kN wheel load (equivalent to just over a 10-tonne axle load).

The main purpose of the research was to cover Task 3 of Stage 2 of the project, which was to analyse the effects of mass on surface texture. However, to relate these finding back to the earlier work on VSD in Stage 1, some additional analysis and modelling of the VSD changes were undertaken. This enables comparisons between the two forms of wear to be made. The important findings are listed below.

5.1 Comparisons of the Wear Models

Texture Models

- The measurement of texture depth has a great deal of variability and it needs to be averaged over a large number of readings to get stable results. Thus getting sensible trends in texture depth changes was not possible by comparing the readings at one measurement station at different numbers of load cycles. The averages had to be taken around a complete cycle of the track.

- The Patrick and the Cenek models for texture change, which are used for pavement performance prediction in New Zealand, do not account well for the effect of mass. These models, which are essentially identical but formulated differently, can be adjusted to match the measured data well, although using coefficients that differ significantly from those given by either Patrick or Cenek.

- A Compaction-Wear model of the form developed for VSD in Stage 1 of this project can be fitted to the texture change data. But because the rate of change of MPD does not appear to become constant, this form of model does not fit the data as well as the Patrick and Cenek models.

- A modification of the form of model used by Kinder & Lay to model surface deformations was fitted to the texture data and resulted in a superior fit to that of the Patrick and Cenek models. As the Kinder-Lay model explicitly accounts for the effect of mass with a power law relationship, it is also much more useful for the aims of this study. The best-fit exponent of the power law for the effect of mass was 1.69.

VSD Models

- The Kinder-Lay form of model was then fitted to the VSD data which had previously been analysed in the Stage 1 report. Fitting models to each of the four pavement segments independently generated good fits, although the fit was not as good as the original Stage 1 Compaction-Wear models. However, the model coefficients for the different segments differed radically from each other even though the pavements were actually quite similar. This severely limits the potential usefulness of these models as a predictive tool because the coefficients cannot easily be determined in advance.

- A single Kinder-Lay model was then fitted to the data for all four segments. This is a much more usable model but did not fit the measured data well for all four pavement segments.

- The Compaction-Wear model developed in Stage 1 had only been fitted to the four segments independently. In Stage 2 a single Compaction-Wear model was fitted to all four pavement segments simultaneously. Although not perfect, this gave a better fit than the Kinder-Lay form of model. The embedded power law term for the effect of mass in this model had an exponent of 1.8.

- The Compaction-Wear model does not account for the load cycles needed to achieve the compaction and thus does not match the initial load cycles well. A blending function with a clear physical interpretation was developed to model this compaction phase and it worked very well.

General Form of Models

- As found in Stage 1, the Compaction-Wear model implies that an increase in mass will result in both additional compaction and additional wear with the effect that an apparent rapid degradation will occur in the condition of the network. Some experimental support for this hypothesis was shown in the measurements undertaken on the pavement in this Stage 2 of the study. The modified Kinder-Lay model used to predict the texture changes does not include an effect similar to this compaction. This does not mean it will not occur but the model cannot predict it, and no experiments have been done that specifically test this hypothesis.

- For both compaction and wear, the power law for the effect of mass has an exponent of just less than 2.

The results should only be interpolated, and should not be extrapolated, outside the range of axle loads that were tested. That is, a power 2 relationship between the 8.2 tonne and 10 tonne axles may not mean that a power 2 relationship can be applied for comparing 6 tonne and 8.2 tonne axles).

5.2 Further Investigations

From these findings some questions for future investigations arise.

- Further experimental validation of the Compaction-Wear model is required. Ideally a pavement at CAPTIF should be loaded at a lower load level until the linear rate of VSD progression is achieved. The load should then be increased and testing continued until the rate of change of VSD stabilises again. This load increase could then be repeated. If the Compaction-Wear model is valid, each load increase should result in additional compaction and an increased wear rate.

- The surface texture should also be tested in a similar manner to VSD and the modified Kinder-Lay model for texture should be validated. If the texture change is a two-stage process like the Compaction-Wear model for VSD, this test will show it.

- Both models have a constant coefficient, K, which depends on the pavement properties. Further work is required to develop methods for predicting the K values from the pavement material properties.

5.3 Applying Pavement Wear Models

Although the Compaction-Wear model may not appear to be substantially different from the power law model currently used, it has major implications when applied to a user pays regime of road funding.

With the Compaction-Wear model a significant part of the total VSD comes from the compaction component which depends on the axle loads but not significantly on the number of load cycles applied.

The compaction component occurs immediately post-construction and therefore the total annual sum collected for compaction could be linked with the total compaction that will occur with pavements constructed in that year.

As the wear component is based on the number of load cycles, it could continue to be collected as road user charges.

Both compaction and wear components are related to approximately the second power of load rather than the fourth power, which means that the relative damage caused by larger trucks with high axle loads would be less than currently assumed. Therefore in the longer term, we would be likely to see a change in the mix of vehicle configurations in the heavy vehicle fleet.

Because this would have a major impact on the road transport industry, the Compaction-Wear model must be suitably validated by further experimentation and testing (as stated in Section 5.2).

6. References

Arnold, G., Alabaster, D.A., Steven, B.D. 2001. Prediction of pavement performance from repeat load tri-axial tests on granular materials. *Transfund New Zealand Research Report No. 214.* 120pp.

AUSTROADS. 1992. *Pavement design: A guide to the structural design of road pavements*. AUSTROADS, Sydney, Australia.

Cebon, D. 1999. *Handbook of vehicle-road interaction.* Swets & Zeitlinger, Lisse, Netherlands.

Cenek, P. 1999. Presentation to the Technical Workshop on dTIMS - 1 June 1999, Wellington. Opus Central Laboratories, Lower Hutt.

de Pont, J. 1997. OECD DIVINE project - Element 1. Longitudinal pavement profiles. *Industrial Research Limited IRL Report No. 708.*

de Pont, J., Steven, B., Pidwerbesky, B. 1999. The relationship between dynamic wheel loads and road wear. *Transfund New Zealand Research Report No. 144.* 88pp.

de Pont, J., Steven, B., Alabaster, D., Fussell, A. 2001. Effect on pavement wear of an increase in mass limits for heavy vehicles. *Transfund New Zealand Research Report No. 207.* 55pp.

Houghton, L.D., Hallett, J.E. 1987. An analysis of single coat seal design. *New Zealand Roading Symposium 2:* 249-263.

ISO. 1997. Characterization of pavement texture by use of surface profile. Part 1: Determination of mean profile depth. *ISO 13473-1:1997.* 19pp. International Standards Organisation (ISO).

Kinder, D.F., Lay, M.G. 1988. Review of the fourth power law. *Australian Road Research Board ARRB Internal Report AIR 000-248.*

OECD. 1998. Dynamic interaction between vehicles and infrastructure experiment (DIVINE). *OECD Technical report IRRD 899920.*

Patrick, J.E., Alabaster, D.J., Dongol, D.M.S. 1998. Pavement density. *Transfund New Zealand Research Report No. 100.*

Pidwerbesky, B.D. 1995. Accelerated dynamic loading of flexible pavements at the Canterbury accelerated pavement testing indoor facility. *Transportation Research Record 1482:* 79-86.

Pidwerbesky, B.D. 1996. Fundamental behaviour of unbound granular pavements subjected to various loading conditions and accelerated trafficking. *University of Canterbury Research Report 96-13.*

Sayers, M.W., Gillespie, T.D., Paterson, W.D.O. 1986. Guidelines for conducting and calibrating road roughness measurements. *World Bank Technical Paper 46.*

Transit New Zealand. 1998. Performance-based specification for bituminous reseals. *Transit New Zealand Specification P17: 1998.*

Vuong, B., Sharp, K. 2001. Impact of heavy vehicles on pavement wear and surfacings: responses-to-load testing using CAPTIF. (AUSTROADS Project No. T. & E.P.N.004. *APRG (AUSTROADS Pavement Reference Group) Report 01/08(LO).* 76pp. ARRB Transport Research Ltd, Vermont South, Victoria, Australia.

Appendix – Surface Texture Data

Loading Cycles	Wheel Path Texture	
	8.2 tonne MPD (mm)	10 tonne MPD (mm)
0	2.35	2.57
1000	2.31	2.45
3000	2.25	2.24
4000	2.27	2.29
5000	2.25	2.25
7500	2.26	2.18
10000	2.20	2.08
15000	2.13	2.09
20000	2.17	2.12
25000	2.12	2.05
30000	2.08	2.01
40000	2.06	1.96
50000	2.04	1.95
70000	1.95	1.91
95000	1.90	1.82
125000	1.89	1.82
150000	1.79	1.83
175000	1.99	1.95